Clim. Past Discuss., https://doi.org/10.5194/cp-2019-23
Manuscript under review for journal Clim. Past
Discussion started: 4 March 2019

Intra-seasonal hydrological processes on the western Tibetan Plateau: Monsoonal and convective rainfall events ~7.5 ka ago.

Linda Taft[a,*], Uwe Wiechert[b], Christian Albrecht[c], Christian Leipe[b], Sumiko Tsukamoto[d], Thomas Wilke[c], Hucai Zhang[e], Frank Riedel[b]

[a]*Department of Geography, University of Bonn, Germany*

[b]*Institute of Geological Sciences, Freie Universität Berlin, Germany*

[c]*Department of Animal Ecology and Systematics, Justus Liebig University Giessen, Germany*

[d]*Leibniz Institute for Applied Geophysics, Hannover, Germany*

[e]*Institute of Plateau Lake Ecology and Pollution Management, Yunnan University, China*

*Corresponding author. E-mail address: ltaft@uni-bonn.de

Keywords

Early Middle Holocene

Bangong Co

Molluscs

Stable isotopes

Abstract

Billions of people depend on the precipitation of the Asian monsoons. The Tibetan Plateau and the Himalayas on the one hand strongly influence the monsoonal circulation pattern and on the other hand represent water towers of humanity. Understanding the dynamics of the Asian monsoons is one of the prime targets in climate research. Modern coupling of atmospheric circulation and hydrological cycle over and on the plateau can be observed and outlined, and lake level controlling factors be identified.

Clim. Past Discuss., https://doi.org/10.5194/cp-2019-23
Manuscript under review for journal Clim. Past
Discussion started: 4 March 2019

Climate of the Past Discussions

Recent monitoring of lakes showed that many of them have grown at least for decades, the causes being higher meltwater inflow or stronger rainfall of different sources, depending on the particular location of a drainage basin. The long-term dynamics, however, can be described best with the aid of high-resolution climate archives. We focus here on the often controversial discussion of Holocene lake development and selected the Bangong Co drainage basin on the western Tibetan Plateau as a case site. The aim of our study is, to identify the factors influencing lake level such as monsoonal or convective precipitation and meltwater. For doing so, shells of the aquatic gastropod genus *Radix* were collected from an early Middle Holocene sediment sequence in the Nama Chu sub-catchment of the eastern Bangong Co and sclerochronlogical isotope patterns of five shells obtained in weekly to sub-monthly resolution. Our data suggests that during ca. 7.5 ka ago, monsoonal rainfall was higher than today. However, summer precipitation was not continuous but affected the area as extended moisture pulses. This implicates that the northern boundary of the SW Asian monsoon was similar to modern times. We could identify convective rainfall events significantly stronger than today. We relate this to higher soil moisture and larger lake surface areas under higher insolation. The regional meltwater amount corresponds with westerly-derived winter snowfall. The snowfall amount was probably similar to modern times. Exceptionally heavy $\delta^{13}C$ values archived in the shells were likely, at least partly, triggered by biogenic methane production. We suggest that our approach is suitable to study other lake systems on the Tibetan Plateau from which fossil *Radix* shells can be obtained. It may thus help to infer palaeo-weather patterns across the plateau.

1. Introduction

1.1. Background and scope

The importance of the Tibetan Plateau and the Himalayas for the Asian atmospheric circulation patterns, particularly their influence on Asian monsoon intensities and distributions, has been demonstrated in numerous studies (e.g. Harris, 2006; Molnar et al., 2009; Boos and Kuang, 2010, Chen et al., 2010). The area represents a water tower furnishing large regions of eastern and southern

Clim. Past Discuss., https://doi.org/10.5194/cp-2019-23
Manuscript under review for journal Clim. Past
Discussion started: 4 March 2019

Asia (Immerzeel et al., 2010; Jacob et al., 2012), and it thus is of major interest to better understand the coupling of atmospheric circulation and the hydrological cycle. Various lake systems on the Tibetan Plateau have been studied with particular focus on Late Glacial and Holocene lake level fluctuations evidencing changes in the hydrological cycle (e.g. Van Campo and Gasse, 1993; Avouac et al., 1996; Lehmkuhl and Haselein, 2000; Ahlborn et al., 2015; Shi et al., 2017; Wünnemann et al., 2018). Accordingly, since the Late Glacial lakes on the plateau were largest during the Early and Middle Holocene and shrank to modern size during the Late Holocene (e.g. Lee et al., 2009; Liu et al., 2013; Shi et al., 2017; in respect of the formal subdivision of the Holocene we follow Walker et al., 2012). In modern times the numerous lakes scattered on the plateau span an area of 30,000 to 50,000 km² (Zheng, 1997; Kong et al., 2007; Ma et al., 2011) but this area was up to four times larger during the Early and Middle Holocene (Hudson and Quade, 2013; Liu et al., 2013).

Recent, mainly satellite-based monitoring suggested that several lakes on the Tibetan Plateau have grown at least since the 1970s (e.g. Liu et al., 2009; Zhang et al., 2011; Lei et al., 2013; Clewing et al., 2014a). In respect of the western Tibetan Plateau, including Ladakh, Hutchinson (1937) concluded that the contemporary lake level rise started already during the late 19th century. Causes might be increase of meltwater inflow (Zhang et al., 2011) or higher monsoonal and/or westerly-derived precipitation (Lei et al., 2013), depending on the particular lake system and its position on the plateau. Kurita and Yamada (2008) discussed the role of local moisture recycling for the precipitation amount and found it significant for the central Tibetan Plateau. The same hydrological factors of lake dynamics on the Tibetan Plateau have to be considered throughout the Holocene (e.g. Gasse et al., 1991; Wünnemann et al., 2010; Bird et al., 2014; Hou et al., 2017). However, they are often controversially discussed against the background that palaeo-moisture sources have to be reconstructed using proxies of different quality (e.g. Taft et al., 2014; Hillman et al., 2017; Wünnemann et al., 2018).

One promising avenue of research to identify palaeo-hydrological processes is the interpretation of stable isotope ratios of carbonatic lake sediments or corresponding carbonate shells (e.g. Mischke et al., 2005; Henderson et al., 2010; Qiang et al., 2017; Liu et al., 2018). Observations of modern processes and analyses of stable isotope behavior in precipitation, rivers and lakes have provided a solid fundament for the interpretation of Tibetan Plateau palaeo-data retrieved from proxies (e.g. Araguás-Araguás, 1998; Pande et al., 2000; Gajurel et al., 2006; Tian, 2007; Hren et al., 2009; Bershaw et al., 2012; Taft et al., 2012; Yao, 2013; Gao, 2014; Mishra et al., 2014; Biggs et al., 2015; He et al., 2015).

It is under discussion whether plateau lakes had an extension during the Middle Holocene similar to that of the Early Holocene (e.g. Liu et al., 2013; Ahlborn et al., 2015; Shi et al., 2017), and when the climate was warmest and most humid (e.g. Morrill et al., 2006; Cheung et al., 2014). There are several studies, however, indicating that the factors controlling lake level may have changed prior to the Late Holocene aridification (e.g. Wei and Gasse, 1999; Bird et al., 2014; Shi et al., 2017). In addition, monsoonal precipitation across the Tibetan Plateau is triggered by SW and SE Asian summer monsoons on the eastern to central plateau while the western plateau is solely influenced by the SW Asian monsoon (e.g. Chen et al., 2015; Ramisch et al., 2016; Wünnemann et al., 2018). Controversial conclusions about the timing of humidity and temperature changes are also due to asynchronous behavior of the different Asian monsoon branches (e.g. An et al., 2000; Wang et al., 2010; Hudson and Quade, 2013). The Holocene climate optimum period was likely earlier on the western plateau than on the eastern plateau (e.g. Wang et al., 2010; Chen et al., 2015).

For Bangong Co, the largest lake system on the western Tibetan Plateau, Gasse et al. (1996) attributed the Holocene lake level changes mainly to changes of the SW Asian summer monsoon. Correspondingly, highest lake levels were assigned to monsoonal moisture maxima during ~9.5 to 8.7 cal. ka B.P. and ~7.2.-6.3 cal. ka B.P. (Fontes et al., 1996; Gasse et al., 1996). Kong et al. (2007), however, concluded that even an enhanced SW Asian monsoon during the Early Holocene did not affect the western Tibetan Plateau significantly. Kong et al. (2007) though referred to Sumxi Co (Fig. 1), a lake system ca. 120 km north of Bangong Co and thus farther from the northernmost monsoon front. Based on a cosmogenic ^{10}Be chronology of the palaeo-shorelines, the authors summarized that high lake levels were most likely associated with increased recharge from melting glaciers. Wünnemann et al. (2010) reported for the neighboring Tso Kar (Fig. 1) that monsoonal precipitation was at maximum from 11.5 to 8.6 cal. ka B.P. but highest lake levels occurred during the early Middle Holocene due to meltwater increase. In respect of nearby Tso Moriri (Fig. 1), Leipe et al. (2014) also suggested that meltwater was the main source to increase the lake level during the Middle Holocene but considered convective rainfall. As mentioned earlier, modern land-atmospheric moisture recycling is known from the Tibetan Plateau (Kurita and Yamada, 2008) and e.g. short-term convective rainfall has been observed over western Tibet and Ladakh (e.g. Gasse et al., 1991; Fontes et al., 1993; personal observations), however, not yet been inferred from Holocene proxies.

The aim of our study is to infer intra-seasonal hydrological processes on the Tibetan Plateau during the Middle Holocene, using Bangong Co as a model site. Which moisture sources were significant for the lake dynamics? How can we differentiate between monsoonal, westerly-derived or convective precipitation and meltwater? Can we distinguish regional convective from monsoonal rainfall, which both occur during the summer months? A potentially suitable, intra-seasonal environmental archive, which is available across the plateau, are the shells of the aquatic gastropod *Radix* (Basommatophora, Lymnaeidae). Taft et al. (2012, 2013) demonstrated that sclerochronological stable isotope patterns from *Radix* shells allow to outline hydrological processes in a sub-monthly resolution.

1.2. Regional setting and study areas

All study sites are located within the Bangong Co drainage basin (Figs. 1 and 2). The basin contains five interconnected lake sub-basins forming the transboundary Bangong Co lake system at 4241 m a.s.l. (SRTM elevation data v4.1; Fig. 2). It comprised a total water surface area of ca. 611 km² in 2012, and stretches ca. 160 km within the western Bangong suture zone (Fig. 1; Fontes et al., 1996, Dortch et al., 2011; Gourbet et al., 2017). Particularly in the eastern Bangong Co lake system, a number of palaeo-shoreline features were observed (e.g. Fontes et al., 1996; Dortch et al., 2011; Clewing et al., 2014a; Fig. 3A), some as high as ca. 80 m above contemporary lake level, witnessing strong past lake level fluctuations and possibly indicating maximum lake extension during the Upper Pleistocene (Shi et al., 2001; Yu et al., 2001). Dortch et al. (2011) suggested a lake level ca. 10 m higher than the modern one during the Early to Middle Holocene, which resulted in a lake area of ca. 810 km^2.

Figure 1

The Bangong Co drainage basin spans an area of ca. 31348 km^2 (including the lake surface area). The mountain ranges, which delimit the watershed, exceed 6000 m a.s.l. (Fig. 1). Cretaceous granodiorites, Cenozoic sandstones and conglomerates, and Late Palaeozoic and Jurassic limestones are widely distributed (Wang and Hu, 2004; Gourbet et al., 2017). Roughly, two thirds of the total catchment area drain into the easternmost basin, Nyak Co (Fig. 2). This causes an overspill of Nyak Co to its neighboring basin. Although Bangong Co has been a closed basin since ca. 7 ka when the palaeo-outflow Tangtse, a river valley connecting to the western terminus of the lake system (Fig. 1), was probably active for the last time (Brown et al. 2003; but compare Dortch et al., 2011), only the westernmost basin behaves like an endorheic lake. Four of the five lakes are overflowing to their neighboring basin in the west (personal observation FR, 2012). While Nyak Co has a relatively low salinity of ca. 0.5 psu, salinity increases significantly along the other basins (Ou, 1981; Wilckens, 2014). This is in phase with $\delta^{18}O_w$, which shows a trend to heavier values towards the west (Wilckens, 2014; Wen et al., 2016).

Figure 2

Table 1

The large alluvial fan of Chiao Ho (Fig. 2A, fossil shells site B) demonstrates long-term low-frequency activity of the northern Nyak Co catchment, which includes meltwater from glaciers (Wei et al., 2015). $\delta^{18}O_w$ of Chiao Ho (Fig. 2A, location 6) was ca. -13,9‰ (Wilckens et al., 2014; Table 1). $\delta^{18}O_w$ from the southern Nyak Co catchment, Makha River (Fig. 2A, location 7) and tributaries, is similar (Fontes et al., 1996; Wilckens, 2014; Wen et al., 2016; Table 1). The eastern catchment of Nyak Co is mainly drained by the Nama Chu and its tributaries (Figs. 2 and 3). The Nama Chu sub-catchment area spans ca. 3420 km^2 (Fig. 1). Hydrological parameters vary stronger here than in the

Clim. Past Discuss., https://doi.org/10.5194/cp-2019-23
Manuscript under review for journal Clim. Past
Discussion started: 4 March 2019

other sub-catchments and are compiled in Table 1 (locations 1-3, in Fig. 2). The Nama Chu and Chiao Ho sub-catchments are in direct neighborhood (Fig. 1).

Figure 3

The Nama Chu valley represents the main study area. Nama Chu represents partly a fluvial system and partly a sequence of ponds (Fig. 3A). We studied the Nama Chu valley from the river mouth at Nyak Co upwards to a saline pond (~30 psu), ca. 28 km from Nyak Co (Figs. 3A, B). The morphology of the valley is controlled by tectonics and alluvial, fluvial and periglacial processes. Alluvial fans, particularly from northern tributaries, block the water flow at several sections leading to the formation of ponds (Fig. 3A; personal observations 2009, 2012). It is likely that during past periods of higher precipitation the general morphology of the fluvio-lacustrine system was similar, based on the assumption that stronger water flow along the Nama Chu was synchronous to stronger lateral alluvial transport into the valley (see Fig. 3A). Field investigation (2012) of sediments exposed in Nama Chu pond basins (e.g. see Fig. 3B) demonstrated that permafrost mounds are widely distributed. They were probably formed by uplift of pond mud, the high water content of which became subject to continuous segregated ice formation (Wünnemann et al., 2008) when the mud became exposed during low water levels.

At the northern edge of the saline pond (triangle in Fig. 2B, camera symbol in Fig. 3A), ca. 4-5 m above the water level, we found sediments containing fossil shells of aquatic molluscs (Fig. 3C). This site is located ca. 45 m above the 2012 lake level of Nyak Co and we conclude that Nyak Co could not capture the palaeo-habitat during its Middle Holocene highstand. Consequently, the palaeo-habitat in Nama Chu can be considered an independent archive of palaeo-precipitation, meltwater events and other hydrological processes. The data from Nama Chu, however, can be scaled up for the Bangong Co drainage basin and partly western Tibet because the general underlying palaeo-hydrological processes were the same or at least very similar.

1.3. Present climate conditions

Clim. Past Discuss., https://doi.org/10.5194/cp-2019-23
Manuscript under review for journal Clim. Past
Discussion started: 4 March 2019

The climate is classified after Köppen-Geiger as cold desert, BWk (Peel et al., 2007). Meteorological data are recorded at a station in Shiquanhe (also referred to as Ali, 32°30'N, 80°05'E, 4285 m a.s.l.), ca. 110 km south of Nyak Co (Fig. 1). Limited data from an automated weather station, set up close to the northern shore of Nyak Co, are in line with those from the station at Shiquanhe (Wen et al., 2016). Precipitation is mainly westerly-derived (Zhang et al., 2011) and convective rainfalls occur (Fontes et al., 1996; personal observation FR, 2012), which amount to 30-40% of the total rainfall (Maussion et al., 2014). Nyak Co is located north but close to the normal northward extension of the SW Asian summer monsoon (Gasse et al., 1991; Fontes et al., 1996; Wu et al., 2006; Tian et al., 2007). Wen et al. (2016) reported a short-term monsoonal rainfall event of 25 mm with $\delta^{18}O$ decreasing rapidly from -9 to ca. -30‰, due to the amount effect in isotope fractionation (e.g. Kurita et al., 2009). The weighted mean of $\delta^{18}O$ in summer precipitation is -14.3‰, and is -18.8‰ in winter (Yao et al., 2013). The $\delta^{18}O$ in precipitation ranges from ca. -30 to -2.5‰ (Wen et al., 2016). Mean annual precipitation is 70 mm (data from 1961 until 2009; Chinese Central Meteorological Office, 2010). Yu et al. (2007) noted 75 mm, Yao et al. (2013) 82 mm. Inter-annual variation can be strong (Wen et al., 2016). The annual potential evaporation can reach almost 2500 mm (Ou, 1981; Wen et al., 2016). The Bangong Co drainage system is located in a permafrost region (Wang and French, 1995; Ran et al., 2015; personal observations). The mean annual air temperature is 0.6°C (data from 1961 until 2009; Chinese Central Meteorological Office, 2010). Minimum monthly temperatures of ca. -20°C occur in January, maximum monthly temperatures are ca. 21°C during July (Ding et al., 2018). The lake is covered by ice from November to April (Wang et al., 2014).

2. Material and methods

2.1. Drainage basin studies and sample sites

Fieldwork was conducted in September 2012. Geomorphology was mainly studied at Nyak Co, along the northern Bangong Co shore as far as the third sub-basin west of Nyak Co, and in the Nama Chu

Clim. Past Discuss., https://doi.org/10.5194/cp-2019-23
Manuscript under review for journal Clim. Past
Discussion started: 4 March 2019

valley (Figs. 1-3). Observations included palaeo-shoreline, alluvial, periglacial and palaeo-glacial features and the water flow direction in the chain of lakes. Electric conductivity, pH and water temperature were measured. Water samples were taken for further analysis to the Freie Universität Berlin. Sites and data of water samples not indicated in Fig. 2 can be found in Wilckens (2014). A geological outcrop at the alluvial fan formed by Chiao Ho (Fig. 2; 33°37.629'N, 79°46.444'E, 4262 m a.s.l. with GPS) exhibited fluvio-lacustrine sediments with well-preserved *Radix* and other shells. A sediment sequence of 1.26 m thickness was sampled in 2 cm steps. The samples of ca. 200 g each were packed in plastic bags and transferred to Freie Universität Berlin for further analyses. In the Nama Chu valley, approximately 28 km east of Nyak Co, well-preserved fossil *Radix* shells were collected from a few cm thick sediment sequence (Figs. 2 and 3; 33°32.018'N, 80°14.176'E, 4297 m a.s.l. with GPS, 4286 m a.s.l. in SRTM) right below and in relation to a palaeo-shoreline. Additional bulk sediment samples were taken for further analysis at the Freie Universität Berlin.

2.2 Geomorphological maps, DEM and CORONA image

The topography in Figs. 1 and 2 is based on 90 m elevation SRTM v4.1 data (Jarvis et al., 2008) acquired year 2000. Catchment and sub-catchment boundaries and the drainage network were also calculated based on the same data set using the Arc Hydro Tools package (ESRI, 2011) in ArcGIS Desktop (ESRI, 2013) following standard workflows summarized in Dartiguenave (2007). Lake, catchment and sub-catchment areas were calculated based on SRTM v4.1 data in a projected coordinate reference system (WGS 84 / UTM zone 44N, EPSG: 32644) in ArcGIS Desktop (ESRI, 2013). Fig. 2 shows the extension and position of water bodies (incl. Nyak Co, dry and water filled basins, and rivers) as of September 2012 according to two Landsat 7 imagery datasets (Entity IDs: LE71460372012267PFS00 and LE71450372012260PFS00, acquired on 2012/09/23 and 2012/09/16, respectively). The CORONA image used in Fig. 3 was purchased from the US Geological Survey (Entity ID: DS1048-1134DA091; coordinates 33.480°N, 79.718°E; camera resolution: stereo medium; acquisition date: 27-SEP-1968).

2.3. Dating

2.3.1. Radiocarbon

A *Radix* shell from the Nama Chu sediment sequence, two *Radix* shells from the Chiao Ho geological outcrop and two charcoal samples from the same Chiao Ho sediment layers (Table 2) were dated at Poznan Radiocarbon Laboratory. Fontes et al. (1996) calculated a lake reservoir effect for Nyak Co of ~6670 years. In the *Radix*-containing sediments from Nama Chu, we could not find charcoal particles or other terrestrial organic remains for correcting the age but at Chiao Ho (Table 2). As Chiao Ho and Nama Chu drain neighboring areas and the distribution of carbonatic rocks is similar in both sub-catchments (Wang and Hu, 2004), we are confident that our age correction makes sense. The similar but independent electron spin resonance (ESR) age supports this conclusion.

2.3.2. Electron spin resonance (ESR)

Preparation and measurements

Radix shell samples from the Nama Chu sediment sequence were gently crushed in a ceramic mortar and sieved with 100 µm to remove finer material. Each aliquot containing 40 mg of the sample was measured with an X-band JEOL FA-100 spectrometer. The measurement parameters used were 324 ± 5 mT magnetic field, 2mW microwave power, 0.1 mT modulation amplitude and scan time of 30s for 5 times. The single aliquot additive dose method was used to calculate the equivalent dose (D_e) using CO_2^- radical signal at g = 2.0006. The irridation of the sample was done with a Varian VF-50J X-ray tube with tungsten target with 50 kV and 1 mA (Oppermann and Tsukamoto, 2015). Aliquots were measured and irradiated within a thin quartz glass tube with 2 mm inner diameter. The sample tubes were sealed with parafilm and were placed upside down during the X-ray irradiation (Tsukamoto et al., 2015).

Calibration of the X-ray dose

The X-ray dose rate for calcium carbonate was calibrated using a modern coral sample. The coral sample was crushed and sieved between 100-150 µm and divided into two sets. One set of the sample coral was irradiated 75.6 Gy from a ^{60}Co gamma source at the Technical University of Denmark. The CO_2^- signal (g =2.0006) from the coral from 3 aliquots of gamma irradiated coral (40 mg) were measured with ESR using the same condition as the shell after preheating at 120°C for 2 minutes. From the unirradiated set 3 aliquots were made and the same signal was measured after X-ray irradiations for 60s and 120s and preheat at 120°C for 2 minutes. The ESR intensity of the gamma irradiation coral was compared with the X-ray dose response curve. The gamma dose of 75.2 Gy is equivalent to 90s X-ray irradiation (Fig. 4a). The X-ray dose rate for calcium carbonate was calculated to 0.84 ± 0.001 Gy/s.

Fig. 4

Equivalent dose measurements

Four natural aliquots of the *Radix* shell were preheated between 100 and 130°C for 2 minutes with a 10°C increment (1 aliquot at each temperature) and the natural CO_2^- radical signal was measured with ESR. Then each aliquot was irradiated with 25 Gy X-ray, preheated at the same temperature and the ESR signal intensity was measured again. This process was repeated 3 times. The D_e values were calculated by extrapolating the dose response curve to zero intensity (Fig. 4b). The D_e values plotted against the preheat temperature are shown in Fig. 4c. The D_e values with preheats between 110 and 130°C are consistent with each other. Therefore, a preheat at 120°C was chosen and 3 more aliquots were measured. The mean D_e value from the 4 aliquots was calculated to 29.5 ± 1.1 Gy (Table 3).

Dose rate and ESR age

Clim. Past Discuss., https://doi.org/10.5194/cp-2019-23
Manuscript under review for journal Clim. Past
Discussion started: 4 March 2019

Climate of the Past Discussions

The external dose rate of the *Radix* shell was estimated using gamma spectrometry. About 5g sediment sample surrounding the shells was sealed within a plastic cylinder about a month to ensure equilibrium between ^{226}Ra and ^{222}Rn. The gamma rays from the sample were then measured using a Well-type high resolution gamma spectrometer. The results are summarized in Table 3. The measured activity of ^{238} U is about twice as large as ^{226}Ra. One possible explanation is that some ^{230}Th has been lost from the ^{238}U decay chain (Long et al., 2014). Therefore, the external dose rate was divided into 2 parts, 1) ‘supported part’ which is originated from ^{232}Th, ^{40}K and the equilibrium part of ^{238}U (calculated from ^{226}Ra activity) and 2) ‘unsupported part’ which is lost at ^{230}Th (calculated based on ^{238}U activity minus ^{226}Ra activity). The beta attenuation factors were calculated based on the thickness of the shell (70-80 µm) and the dose rate conversion factors of Guérin at al. (2011) were used. An alpha dose efficiency of 0.1 ± 0.05 was assumed (e.g. Skinner, 1989). The cosmic dose rate was calculated following Prescott and Hutton (1994).

Table 3

2.4. Sediment processing and assignment and documentation of molluscan shells

The sediment samples were washed and sieved using mesh sizes of 1, 0.5, 0.25 and 0.1 mm. The sieved residue was visually analyzed using a Zeiss stereo microscope SV8. Shells of gastropods and bivalves were picked for palaeo-environmental reconstruction and tiny pieces of charcoal were separated for radiocarbon dating. Some shells were photographed using a Keyence VHX-1000 microscope (e.g. Fig. 5).

2.5. Stable isotopes

Five *Radix* shells from the Nama Chu site (Figs. 2 and 3) were selected for stable isotope analysis based on shell preservation, completeness and sizes (Table 5; Fig. 5). *Radix* shells are built from aragonite (e.g. Taft et al., 2012, 2013). First, the shells were cleaned in an ultrasonic bath and subsequently any residual sediment particles were removed manually with a small brush. Sub-sampling was conducted using a special dental drill device for milling the outer primary shell layer in a constant distance along the ontogenetic order of the shell increments with a maximum depth of 50 µm. Up to 38 sub-samples were obtained from a single shell (Table 5), labeled in alphabetical order, with [a] representing the ontogenetically latest shell part at the outer rim. The sub-samples of ~150 µg were then measured for $\delta^{18}O$ and $\delta^{13}C$ ratios using a GasBench II linked to a MAT-253 ThermoFischer Scientific™ isotope ratio mass spectrometer at Freie Universität Berlin. The measurements were standardized against Carrara Marble (CAM) and Kaiserstuhl carbonatite in-house reference material (KKS), which had been calibrated against Vienna PeeDee Belemnite (V-PDB) international isotope reference material using NBS-18 and NBS-19. All results are reported in δ notation relative to V-PDB. The external error (simple standard deviation) of the measurements is ± 0.06‰ for $\delta^{18}O$ and ± 0.04‰ for $\delta^{13}C$.

3. Results

3.1. Dating

3.1.1. Radiocarbon

A *Radix* shell sampled from the Nama Chu sediment layer was dated to 12670 ± 60 years B.P. Two *Radix* shells from the Chiao Ho alluvial section were dated to 8540 ± 40 and 8480 ± 40 years B.P. Two charcoal samples from the same Chiao Ho sediment layers were dated to 2275 ± 30 and 2400 ±30 years B.P. The ^{14}C ages of the two charcoal samples were subtracted from the ages of the two Chiao Ho *Radix* shells. Consequently, the lake reservoir effects for the latter shells are 6265 and 6080 ^{14}C years B.P. A mean lake reservoir effect of 6172 ^{14}C years B.P. was then subtracted from the age of the Nama Chu shell which results in 6498 years B.P. Calibration of 6498 years B.P. with CALIB (Stuiver et al., 2013, online executive version 7.0html) resulted in a weighted average age at 2σ precision of

Clim. Past Discuss., https://doi.org/10.5194/cp-2019-23
Manuscript under review for journal Clim. Past
Discussion started: 4 March 2019

7393 ± 114 cal. years B.P. The radiocarbon age of the Nama Chu sediment horizon is therefore considered ~7.4 ± 0.1 cal. ka B.P., which is early Middle Holocene. The data are compiled in Table 2.

Table 2

3.1.2. Electron spin resonance

The internal U content of the fossil *Radix* sample from Nama Chu was not measured. The U content of modern *Radix* shells from Bangong Co was measured and the mean value is 0.05 ± 0.01 (n = 6; Wassermann, 2014). However, it is well known that shells take up U from surroundings (e.g. Grün, 1989). Schellmann et al. (2008) reported a mean U content of Holocene shells (> 2.5 ka) to be 2.8 ± 2.7 ppm (n = 63). Assuming this mean U content as the current U content of the shells, we calculated the age by two scenarios: U content increased linearly with time (linear uptake, LU) or the uptake occurred at an early stage of the burial time (early uptake, EU). The calculated ages are 8.1 ± 1.0 ka (LU) and 7.4 ± 1 ka (EU) respectively (Table 3).

Table 3

3.2. Features of the early Middle Holocene habitat inferred molluscan shells

The sandy to fine-gravelly deposits sampled at a Nama Chu pond palaeo-shoreline (Fig. 3) exhibited shells from four molluscan genera (Fig. 3C). Shells of the aquatic gastropods *Radix* sp. and *Gyraulus* sp. were fairly abundant. In comparison, shells of the bivalve *Pisidium* sp. occurred less frequently and from the gastropod *Valvata* sp. only single shells were found. The ecological traits of these genera, which provide information about the palaeoenvironment, are compiled in Table 4.

Table 4

3.3. Shell morphology and $\delta^{18}O$ and $\delta^{13}C$ values in early Middle Holocene Radix

Prior to sub-sampling (micro-milling), the selected five shells, termed NC1-5, were measured in height and the number of whorls were counted. These data and the individual number of sub-samples are compiled in Table 5. As an example, the shell NC2 is figured (Fig. 5).

Fig. 5

Table 5

All sclerochronological isotope patterns and single isotope values are shown in Fig. 6 and Table 6, respectively. The range of $\delta^{18}O$ values in all five shells that were analyzed, is from -10.2‰ in shell NC3 to -2.5‰ in shell NC5. The mean oxygen isotope compositions of shells NC1-4 are in the range between -9.2 and -7.5‰. Shell NC5 exhibits a mean $\delta^{18}O$ value of -4.6‰. The range of $\delta^{13}C$ values in all five shells analyzed is from 3.2‰ in NC4 to 8.4‰ in NC1. The mean carbon isotope values of the shells are in the range of 4.9 to 6.5‰. The correlations between oxygen and carbon stable isotope patterns are r^2= 0.8 for NC1, 0.5 for NC2 and NC3, 0.4 for NC4 and 0.8 for NC5.

Fig. 6

Table 6

4. Discussion

4.1. Age of Radix *shells*

Two dating methods were applied; radiocarbon, which produced an age for the Nama Chu shells of ~7.4 ± 0.1 cal. ka B.P., and electron spin resonance, which gave an age of 8.1 ± 1 ka (LU model) and

7.4 ± 1 ka (EU model). The inferred lake reservoir effect of ~6200 years suggests strong detrial input of old carbon. Fontes et al. (1996) calculated a lake reservoir effect of 6670 years for a sediment core taken from central eastern Nyak Co. On the one hand this difference of ~500 years does not significantly increase temporal uncertainty of our early Middle Holocene case study and on the other hand it could be due to higher detrial input of Jurassic limestone by the Makha River (Fig. 2), which is draining the southern catchment of Nyak Co. The EU-model-ESR age of 7.4 ± 1 ka is very similar to the radiocarbon age of 7.4 ± 0.1 ka. We thus tentatively consider an approximate age of ~7.5 ka to address the palaeo-habitat and are confident to report early Middle Holocene processes. Although the five shells used for stable isotope analyses came from a single few cm thick sediment layer, we assume that they rather reflect a multi-decadal period, and thus represent environmental archives of five different years. This assumption is supported by the sclerochronological stable isotope patterns (Table 6; 4.3.).

4.2. Habitat simulation with the aid of early Middle Holocene aquatic molluscs

The fossil assemblage indicates a shallow littoral environment (Table 4). This is in line with the observation that the sediments were deposited along a palaeo-shore. We therefore use the palaeo-shoreline as contemporary water level (Fig. 2C). Considering the reconstruction of Dortch et al. (2011) that the Early to Middle Holocene lake level of Nyak Co was ca. 10 m higher than nowadays, the difference to the level of the Nama Chu pond was ca. 35 m. When the pond was filled up to the palaeo-shoreline, it was approximately 5-6 m deep and interconnected with the neighboring ponds (Fig. 2C). The short-term grain size changes, e.g. from fine sand to fine gravel, show that there were significant hydrological changes, but generally it can be assumed that it was a lacustrine to semi-lacustrine habitat. Salinity was in the range of freshwater to oligohaline (Table 4).

4.3. $\delta^{18}O$ and $\delta^{13}C$ values in shells from early Middle Holocene Radix *shells*

4.3.1. Mean values and range of values

The range of mean $\delta^{18}O$ values of the five shells from -9.2 to -4.6‰ indicates that the Nama Chu palaeo-habitat was located in a dynamic hydrological system. This becomes even more evident when comparing the most negative (-10.2‰) and the least negative (-2.5‰) values. Modern shells from Nyak Co have mean values of -2.18 and -2.23‰ (Taft et al., 2013). Several authors who studied precipitation or aquatic systems on the plateau (e.g. Fontes et al., 1996; Cai et al., 2012; Wünnemann et al., 2018) have argued that not temperature but precipitation source and amount, and evaporation are the dominant factors in oxygen isotope fractionation. Based on precipitation recorded at Shiquanhe (Fig. 1), Yu et al. (2007), however, concluded that variations in $\delta^{18}O$ relate closely to temperature variations. Bangong Co water, on the other hand, was considered to be mainly controlled by local relative humidity (Wen et al., 2016). We interpret the lower $\delta^{18}O$ values of Nama Chu compared to Nyak Co primarily as an effect of shorter water residence time, i.e. the water is less influenced by evaporation. Mean -9.2‰ indicates a significantly stronger water flow than mean -4.6‰. The range reflects semi-lacustrine to lacustrine conditions. A correlation of r^2= 0.8 between oxygen and carbon stable isotope values (Table 6) in shells NC1 (mean $\delta^{18}O$ of -7.5‰) and NC5 (mean $\delta^{18}O$ of -4.6‰) indicates some degree of covariance, which is typical for closed-basin lakes and ponds (Li and Ku, 1997; Taft et al., 2013). The closed-basin periods, however, likely did not last for long because the freshwater molluscan assemblage demonstrates that salinity did not vary much. On the other hand, modern shells from Nyak Co show rather low $\delta^{18}O$, which co-varies with $\delta^{13}C$ (Taft et al., 2013), indicating a closed basin but the lake spills over to its neighboring basin and salinity is low. The water sources of the Nama Chu palaeo-habitat are discussed under 4.3.2.

Mean $\delta^{13}C$ values of the five shells are in a range of 4.9 to 6.5‰, which is exceptionally positive, compared to other (semi-) lacustrine systems (e.g. Leng and Marshall 2004) but in line with $\delta^{13}C_{DIC}$ from modern sediments of the Nama Chu pond (Table 1). Shells of *Radix* sp. living in Nyak Co show mean $\delta^{13}C$ values of -2.35 and -2.48‰ (Taft et al., 2013). Fontes et al. (1996), however, reported $\delta^{13}C$ values from early Holocene Nyak Co carbonates of up to 7.2‰, which they related to enhanced aquatic photosynthesis during evaporative shallow lake conditions and/or to some methane formation within bottom sediments. Other regional high $\delta^{13}C$ values were found in Sumxi Co (Fig. 1)

Clim. Past Discuss., https://doi.org/10.5194/cp-2019-23
Manuscript under review for journal Clim. Past
Discussion started: 4 March 2019

carbonates (Fontes et al., 1993) and in a Tso Moriri (Fig. 1) sediment core (Mishra et al., 2015). The latter authors concluded that the role of phytoplankton productivity was minimal because of oligotrophic conditions (Mishra et al., 2015). Goto et al. (2003) reported similar high $\delta^{13}C$ values from central Tibetan Plateau Siling Co, which they related to evaporation (Stiller et al., 1985). The even more positive $\delta^{13}C$ values of carbonates from Lake Caohai (China, Guizhou Province) were explained by bacterial degradation of aquatic organic matter, generating methane, preferentially $^{12}CH_4$, and leading to an enrichment of ^{13}C in the lake water and carbonate (Zhu et al., 2013).

We consider that the high $\delta^{13}C$ values were likely triggered by a combination of the cited factors plus detrial input. Effective evaporation is reflected by corresponding $\delta^{13}C$ and $\delta^{18}O$ values (Horton et al., 2016). The most negative $\delta^{18}O$ value is from the same shell as the least positive $\delta^{13}C$ value; the least negative $\delta^{18}O$ value is from the same shell as the most positive $\delta^{13}C$ value; etc. Organic productivity was probably higher than in Nyak Co, due to the fact that the Nama Chu pond was only 5-6 m deep, and light could penetrate to the bottom and trigger photosynthetic processes in all water layers. Aquatic plants and algae utilize CO_2 as source of carbon for photosynthetic processes with preferable uptake of ^{12}C (Chikaraishi, 2014), which leads to a ^{13}C enrichment. Methane bubbling was observed (2009, 2012) and it is likely that organic-rich mud was available for microbes also during the early Middle Holocene. Liu et al. (2017) outlined methanogenic pathways from a short Nyak Co sediment core. $\delta^{13}C_{CH4}$ was in a range of ca. -60 to -110‰. Seasonal permafrost thawing could have triggered another methanogenic pathway (Rivkina et al., 2007). Permafrost represents a considerable carbon pool (Wagner et al., 2007; Mackelprang et al., 2011). Methane bubbling means that preferably ^{12}C was removed from the Nama Chu palaeo-habitat, leaving the remaining carbon ^{13}C enriched (Walter et al., 2006). Detrital input of old carbon from Jurassic and Permian limestone (Wang and Hu, 2004) is considered to represent another cause for the high $\delta^{13}C$ values. The limestones probably represent shallow water tropical carbonate formations which may exhibit $\delta^{13}C$ values as positive (e.g. Isozaki et al., 2007) as was measured in the fossil *Radix* shells. The relatively high ^{14}C reservoir effect in the Bangong Co system (Fontes et al, 1996; this study) indicates detrital input of old carbon.

4.3.2. Sclerochronological patterns

Clim. Past Discuss., https://doi.org/10.5194/cp-2019-23
Manuscript under review for journal Clim. Past
Discussion started: 4 March 2019

The palaeo-environmental setting suggests that the Nama Chu pond was sensitive to short-term atmospherical, hydrological, limnological and hydromorphological changes. It thus can be expected that the five *Radix* shells, which were formed in equilibrium with the pond water, archive early Middle Holocene hydrological signals over their life spans of ca. 12-15 months (Taft et al., 2012, 2013). The sediment sequence from which the shells were sampled represents a multi-decadal period, and the individual ranges of stable isotopes and their mean values (4.3.1.) indicate that the five shells reflect five different years around ~7.5 ka. The interpretation of isotopic signatures of the shells is based on the following considerations:

a) Precipitation source: Regional monsoonal (summer) precipitation has mean $\delta^{18}O$ values of ca. -14 to -16‰ (Yu et al., 2007; Yao et al., 2013) and can be as low as -30‰ in case of short-term heavy rainfall (Wen et al., 2016). Monsoonal rainfall is therefore isotopically lighter than the pond water and negative excursions can be expected in the isotope patterns of the shells. Convective clouds form by regional moisture evaporation particularly during May to October when the lake surfaces are not covered by ice. Seasonal permafrost thawing provides soil moisture, which becomes part of the convective system. Potential monsoonal rainfall would add to the soil moisture. Measured $\delta^{18}O$ values of regional convective rainfall range from ca. -5.5 to 0.2‰ (Fontes et al., 1996; Mishra et al., 2014) and thus at least in shells NC1-4 positive isotopic excursions can be expected, in case of a significant amount. June snowfall over Tso Moriri (Fig. 1) exhibited a $\delta^{18}O$ value of -22.4‰ (Biggs et al., 2015). Regional snowfall accumulates mainly in winter and is westerly-derived (Biggs et al., 2015). The oxygen isotope composition of local rivers is dominated by meltwater and ranges from ca. -12 to -14‰ in the Nyak Co catchment (Fontes et al., 1996; Wilckens, 2014; Wen et al., 2016). Meltwater pulses thus will lead to negative excursions in $\delta^{18}O$ patterns of the Nama Chu shells. Regional meltwater increases in May and peaks in July (personal communication with local people, 2012). In the case of Nama Chu snowmelt and permafrost thawing have to be considered.

b) Precipitation amount: Quantification is difficult but rainfall, which is intensive enough to wash in soil, can be identified using $\delta^{13}C$ (Taft et al., 2012, 2013). $\delta^{13}C$ of dissolved soil carbonate from Ladakh revealed values from ca. -20 to -28‰ (Longbottom et al., 2014). Dissolved organic carbon from terrestrial plants is in a similar range (Cloern et al., 2002; Wynn et al., 2007). The mean $\delta^{13}C$ values of the Nama Chu shells range from 4.9 to 6.5‰. Carbon washed in from soil thus would lead to negative isotope excursions in the sclerochronological patterns.

c) Evaporation and ice cover period: From November to April, Nyak Co is covered by ice (Wang et al., 2014), and it can be assumed that the surface of the Nama Chu palaeo-pond was frozen for a similar period although possibly with a seasonal lag of some weeks due to the lower water depth. The ice cover period may have been shorter during the early Middle Holocene. Ice cover prevents exchange between atmosphere and pond water, and potential changes in isotope composition must be intrinsic. Consequently, variation of oxygen isotope values is considered to be low during ice cover conditions, carbon isotope values, however, decrease due to reduced productivity under lower light penetration and lower temperatures. Evaporation is effective from approximately May to October and leads to heavier isotope values but is potentially superimposed by meltwater inflow and rainfall. The effect of evaporation can be seen best regarding the dry period after summer rainfall until the beginning of ice cover (Taft et al., 2013). The mean isotope values of the shells (Table 6), however, show clearly the inter-annually varying influence of evaporation.

d) Organic productivity: Main controlling factors are light and temperature (Chikaraishi, 2014) and thus periodically higher $\delta^{13}C$ shell values reflect the summer season while lower $\delta^{13}C$ shell values indicate reduced productivity of water plants and algae during winter. The productivity of microbes is exemplified by archaeans and briefly outlined in the next paragraph.

e) Methanogenesis: During biogenic methane production preferably ^{12}C is processed (Walter et al., 2006). While the gas will leave the habitat by bubbling during the summer months triggering ^{13}C enrichment in the water, it may accumulate under ice in winter. It was observed (FR, 2013) on the eastern Tibetan Plateau that *Radix* moves on the underside of pond ice and likely consumes algal growth there. Thus it can be expected that methanogenesis is occasionally archived in *Radix* shells. Recent observation (2009, 2012) of methane bubbling in the Nama Chu pond hints at this possibility.

f) Temporal resolution: Although *Radix* is active in all seasons and even under ice, it grows much slower in winter than in summer (Gaten, 1986). Data from modern *Radix* shells indicate that growth was ca. three times slower during the ice cover period compared to the average ice-free period

(Taft et al., 2013). The temporal resolution of the summer isotopic signals archived in the shell is thus significantly higher (ca. weekly) than of those archived in winter.

It is unlikely that the five early Middle Holocene *Radix* individuals hatched and died during the same time of a year but represent records of different length and seasonality. Maximum shell height and number of whorls are notably lower in NC5 (Table 5) suggesting that this individual had a comparatively shorter lifespan. Ice cover periods identified in the isotope patterns can, for example, be used to infer the chronology of the individual isotope patterns. The ice cover period in shell NC2 (Fig. 6) is from [t] to [p]. $\delta^{18}O$ shows little variation in this shell section and $\delta^{13}C$ values are relatively low. Interestingly $\delta^{13}C$ increases temporarily around [s]. We speculate that methanogenesis was responsible for this effect. A similar $\delta^{13}C$ excursion can be seen in shell NC1 (Fig. 6) where the ice cover period is from [p] to [k] and is even more significant (double peak) in shell NC3 where the ice cover period is from [q] to [l]. In shell NC4, $\delta^{18}O$ shows little variation from [t] to [a], which is much too long a period for ice cover, suggesting superimposition by other factors. The lowest $\delta^{13}C$ values imply that ice cover was roughly from [s] to [n]. In shell NC5, we tentatively appoint the ice cover period to [o] to [k]. $\delta^{18}O$ shows little variation and $\delta^{13}C$ values are low here. Using this seasonal marker, we discuss the complete isotope patterns of NC1-5 in ontogenetic chronology (Fig. 6).

Shell NC1: This gastropod hatched during early summer. The general trend of $\delta^{13}C$ shows increasing productivity to [w], which is overprinted by two negative excursions, with minimum values at [z10] and [z2]. During the first negative $\delta^{13}C$ excursion, $\delta^{18}O$ decreases correspondingly. We interpret this as significant monsoonal precipitation, bringing isotopic lighter rain into the pond and triggering the inwash of isotopically light soil carbon. The second negative $\delta^{13}C$ excursion is accompanied by a positive $\delta^{18}O$ peak at [z3]. Again a significant inwash of soil carbon occurred but this time triggered by convective rainfall. The following increase of $\delta^{18}O$ to [x] is considered to reflect the dominance of evaporation, which is in line with the increasing $\delta^{13}C$ values. The subsequent shift to lighter stable isotope values represents the transition to winter conditions, with reduced evaporation and decreasing primary bioproductivity. The ice cover period from [p] to [k] is followed by an increase of bioproductivity until again summer conditions were reached. $\delta^{18}O$ was strongly dominated by evaporation suggesting that there was little snowfall during the preceding winter and thus no significant influence by meltwater. The gastropod died before potential (second) summer rainfall events occurred. Occasional light rain could have fallen but cannot be detected in the isotope pattern because of signal weakness.

Shell NC2: This gastropod hatched when significant monsoon moisture penetrated the western Tibetan Plateau, likely during middle summer. Indication are negative excursions of $\delta^{18}O$ [z7] and $\delta^{13}C$ [z6]. Inwash of light terrestrial carbon stopped immediately with the termination of heavy rainfall leading to a steep increase of $\delta^{13}C$ to the high summer bioproductivity level [z3]. The subsequent increase of $\delta^{18}O$ to [z3] is due to evaporation dominating potential lighter rainfalls and snowmelt. A second monsoonal rainfall period is indicated by abrupt decreases at [z2] of $\delta^{13}C$ and $\delta^{18}O$. The following steep increase of $\delta^{18}O$ is due to evaporation and likely represents September, when rainfall amounts were low and meltwater played a minor role, due to lower temperatures. Such a September pattern was found in modern *Radix* sp. from Nyak Co (Taft et al., 2013). The subsequent turnover of isotope signatures to lighter values can be explained by increasingly weaker insolation and colder temperatures, likely during October ~7.5 ka. In November the pond became ice covered ([t] to [p]). The following spring (May) primary bioproductivity increased quickly and the pattern shows no negative excursions until [b]. The simultaneous increase of $\delta^{18}O$ is modest to [e] but stronger afterwards to [b], likely because the evaporation signal could dominate the meltwater signal only in summer. The synchronous abrupt negative excursions in $\delta^{13}C$ and $\delta^{18}O$ from [b] to [a] may indicate a monsoonal moisture pulse.

Shell NC3: This *Radix* individual hatched in early summer when primary bioproductivity started to increase significantly. A small negative excursion of $\delta^{13}C$ and an even smaller negative peak of $\delta^{18}O$ at [z2] may represent a monsoonal moisture pulse. With a mean of -9.2‰, $\delta^{18}O$ of the pond was relatively negative and thus monsoonal rainfall is likely not well evidenced in the pattern. The negative $\delta^{18}O$ peak at [x] is considered a meltwater pulse and not heavy rainfall because $\delta^{13}C$ did not react. $\delta^{13}C$ and $\delta^{18}O$ peak at [u], likely in September. Autumn turnover is indicated by steep decreases of $\delta^{13}C$ and $\delta^{18}O$ towards the ice cover period [q] to [l]. Spring (May) is characterized by increasing

$\delta^{13}C$ and $\delta^{18}O$ values to [e]. A simultaneous drop of both isotope values to [c] may exhibit a monsoonal moisture pulse.

Shell NC4: This snail hatched in late summer because primary bioproductivity was already quite high. The period to [z] may represent September because of evaporation dominating $\delta^{18}O$. In September ~7.5 ka, just before the autumn turnover started, strong convective rainfall is evidenced by $\delta^{18}O$ becoming heavier and the abrupt negative excursion of $\delta^{13}C$. Autumn (October) turnover is clearly indicated by decreasing stable isotope values towards the ice cover period which was likely from [s] to [n]. The following spring (May) is characterized by increasing bioproductivity, $\delta^{18}O$, however, showing a negative trend. This may be explained by meltwater dominating evaporation. It is possible but unlikely that the negative excursion of $\delta^{13}C$ at [b] was caused by rainfall because $\delta^{18}O$ of the pond water remained unchanged at ca. -8‰, and rainfall with similar values is difficult to infer for the region as no such value has been reported.

Shell NC5: This individual hatched in late summer when evaporation became dominant and primary bioproductivity reached its maximum. The simultaneous negative peaks of $\delta^{13}C$ and $\delta^{18}O$ at [r] indicate a September monsoonal moisture pulse. September is inferred because of the evaporation signal still increasing due to rainfall/humidity ceasing. On the other hand, bioproductivity had started to decrease. The autumn turnover terminated with the beginning of the ice cover period which is approximately from [o] to [k]. The following spring (May) triggered bioproductivity ($\delta^{13}C$) and evaporation began dominating the $\delta^{18}O$ values to [d]. Subsequently, both isotope values drop, which we consider the pattern of monsoonal moisture penetration into the area (Fig. 6).

Four out of five of the sclerochronological stable isotope records exhibit significant rainfall periods. In shell NC3 the signals are less clear, which might be due to the generally lighter $\delta^{18}O$ of the palaeo-pond water. Five to eight rainfall events are related to monsoonal moisture, while two events evidence strong convective rainfall. Shell NC2 indicates that two monsoonal moisture pulses could appear during one season. Isotope patterns of modern *Radix* shells from lake basins with regular monsoonal precipitation, Bangda Co and Donggi Cona (eastern Tibetan Plateau), reveal single extended events, relating to the summer rain season (Taft et al., 2012, 2013). The monsoonal behavior in the study area

Clim. Past Discuss., https://doi.org/10.5194/cp-2019-23
Manuscript under review for journal Clim. Past
Discussion started: 4 March 2019

Climate of the Past Discussions

on the western Tibetan Plateau was thus quite different. The data suggest that during the early Middle Holocene the monsoonal moisture did not penetrate much further onto the plateau than nowadays, with the difference, rainfall events/periods happened more regularly and were stronger. Two shell patterns (NC1, NC4) indicate convective rainfall, which we consider stronger or more extended than those observed in modern times. This can be explained by higher summer insolation (Berger and Loutre, 1991), moister soils due to monsoonal precipitation and much more extended lake surfaces (Liu et al., 2013) around ~7.5 ka. The average annual precipitation amount was likely several times higher than nowadays. These suppositions are basically in line with other early Middle Holocene records from the western plateau (Gasse et al., 1991, 1996; Fontes et al., 1993; Brown et al., 2003; Wünnemann et al., 2010).

There are no glaciers located in the Nama Chu catchment and there is no indication that it was different under early Middle Holocene climate. The amount of meltwater that reached the palaeo-pond was therefore mainly dependent on westerly-derived snowfall during winter. Summer snowfall occurs nowadays but snow normally melts within hours to a couple of days (personal observations) and thus does not add to spring meltwater from accumulated winter snowfall. These processes unlikely changed during the Holocene. The role of seasonal permafrost thawing for the hydrological system remains unclear. The five shell patterns indicate inter-annual differences in meltwater amounts. While in shells NC1 and NC5 little influence of meltwater on $\delta^{18}O$ can be inferred, the influence is significant in shell NC2, the isotopically light meltwater mitigating the evaporation signal during spring and early summer. The strong meltwater pulse identified in NC3 can be possibly related to the outburst of a meltwater-fed pond in the upper catchment of Nama Chu. The domination of meltwater in the isotope pattern of NC4 is in line with the pattern of a modern *Radix* from southern Nyak Co (Taft et al., 2013), sampled not far from the mouth of the Makha River (Fig. 2), which is draining meltwater (personal observation FR, 2012). Based on our data, we suggest that the westerly influence during ~7.5 ka winters was similar to modern times.

The ice cover period during ~7.5 ka was recorded by all shells. The data, however, do not allow to infer whether the length of the ice cover period differed from the modern situation. This is

Clim. Past Discuss., https://doi.org/10.5194/cp-2019-23
Manuscript under review for journal Clim. Past
Discussion started: 4 March 2019

also due to the weak observational record for comparison and that we do not have a good modern analogue for the Nama Chu palaeo-pond.

The influence of biogenic methane production on $\delta^{13}C$ is likely, due to the high mean values in the context of methane bubbling observation. On the other hand, specific positive excursions during the ice cover period, cannot easily be explained by primary producers' productivity pulses. We consider the influence of methane production on the $\delta^{13}C$ of certain ponds or lakes underestimated.

5. Conclusions

The sclerochronological isotope patterns of early Middle Holocene *Radix* shells are suitable to report hydrological processes from the western Tibetan Plateau in ca. weekly (summer) to sub-monthly (winter) resolution over the lifespan of the gastropod, which is about one year.

We infer from our data that i) monsoonal rainfall reached the area more regularly and in higher amounts than nowadays; ii) monsoonal rainfall did not prevail over the whole summer season but penetrated the western Tibetan Plateau as extended moisture pulses; iii) the northern boundary of the SW Asian summer monsoon was in a similar position as in modern times but the monsoonal system was more dynamic; iv) significant convective rainfall occurred and can be clearly distinguished from monsoonal precipitation with the aid of stable isotope patterns; significant convective rainfall is due to higher summer insolation (evaporation), higher soil moisture (by monsoonal penetration) and much larger lake surface areas during ~7.5 ka; v) isotopic signals of monsoonal and regional convective precipitation can be clearly differentiated from meltwater signals in the records; vi) in the study area, the meltwater amount correlates with westerly-derived winter snowfall amount; the snowfall amount during the early Middle Holocene was probably similar to modern times; vii) biogenic methane production could likely be identified in the isotope patterns and is possibly underestimated in lake systems.

Author contribution

LT and FR prepared the original manuscript with contributions from all co-authors. FR conceptualized the overarching research goals and aims. ST developed the design of the dating methods. LT and UW performed and interpreted the stable isotope data. HC was responsible for the coordination of the research activity planning and execution. CA and TW investigated the ecological traits of the molluscs. CL was responsible for the visualization and presentation of the data.

Acknowledgements

Catharina Clewing (Giessen University, Germany) and Marc Weynell (FU Berlin) greatly assisted Frank Riedel during fieldwork on the western Tibetan Plateau in 2012. We appreciate that Maike Glos (FU Berlin) processed the sediments. She also micro-milled the gastropod shells and prepared the samples for stable isotope analyses. Many thanks to Atsushi Suzuki (Geological Survey of Japan) and Mayuri Inoue (Okayama University) who provided the modern coral sample for the X-ray calibration for ESR dating. The gamma irradiation was made with the help of Jakob Helt-Hansen, Jim Thorslund Andersen and Kristina Thomsen (all Technical University of Denmark). Thanks to Tomasz Goslar (Poznan, Poland) for determination of the radiocarbon ages. Jan Evers (FU Berlin) kindly improved figures. We are grateful to the German Science Foundation (DFG) for financial support. This is a contribution to the DFG priority program TiP.

References

Ahlborn, M., Haberzettl, T., Wang, J., Fürstenberg, S., Mäusbacher, R., Mazzocco, J., Pierson, J., Zhu, L., Frenzel, P.: Holocene lake level history of the Tangra Yumco lake system, southern-central Tibetan Plateau, The Holocene, 26, 176-187, 2015.

An, Z., Porter, S.C., Kutzbach, J.E., Wu, X., Wang, S., Liu, X., Li, X., Zhou, W.: Asynchronous Holocene optimum of the East Asian monsoon, Quaternary Sci Rev, 19, 743-762, 2000.

Araguás-Araguás, L., Froehlich, K., Rozanski, K.: Stable isotope composition of precipitation over southeast Asia, J Geophys Res, 103, 28721-28742, 1998.

Clim. Past Discuss., https://doi.org/10.5194/cp-2019-23
Manuscript under review for journal Clim. Past
Discussion started: 4 March 2019

Avouac, J.P., Dobremez, J.F., Bourjot, L.: Palaeoclimatic interpretation of a topographic profile across middle Holocene regressive shorelines of Longmu Co (western Tibet), Palaeogeogr Palaeocli, 120, 93-104, 1996.

Berger, A., Loutre, M.F.: Insolation values of the last 10 million years, Quaternary Sci Rev, 10, 297-317, 1991.

Bershaw, J., Penny, S.M., Garzione, C.N.: Stable isotopes of modern water across the Himalaya and eastern Tibetan Plateau: Implications for estimates of paleoelevation and paleoclimate, J Geophys Res, 117, D02110, 2012.

Biggs, T.W., Lai, C.T., Chandan, P., Lee, R.M., Messina, A., Lesher, R.S., Khatoon, N.: Evaporative fractions and elevation effects on stable isotopes of high elevation lakes and streams in arid western Himalaya, J Hydrol, 522, 239-249, 2015.

Bird, B.W., Polisar, P.J., Lei, Y., Thompson, L.G., Yao, T., Finney, B.P., Bain, D.J., Pompeani, D.P., Steinman, B.A.: A Tibetan lake sediment record of Holocene Indian summer monsoon variability, Earth Planet Sc Lett, 399, 92-102, 2014.

Boos, W.R., Kuang, Z.M.: Dominant control of the South Asian monsoon by orographic insulation versus plateau heating, Nature, 463, 218-223, 2010.

Brown, E.T., Bendick, R., Bourlès, D.L., Gaur, V., Molnar, P., Raisbeck, G.M., Yiou, F.: Early Holocene climate recorded in geomorphological features in Western Tibet, Palaeogeogr Palaeoclim, 199, 141-151, 2003.

Burky, A.J., Hornbach, D.J., Way, C.M.: Growth of *Pisidium casertanum* (Poli) in west central Ohio, Ohio J Sci, 81, 41-44, 1981.

Cai, Y., Zhang, H., Cheng, H., An, Z., Edwards, R.L., Wang, X., Tan, L., Liang, F., Wang, J., Kelly, M.: The Holocene Indian monsoon variability over the southern Tibetan Plateau and its teleconnections, Earth Planet Sc Lett, 335-336, 135-144, 2012.

Chen, F., Chen, J., Holmes, J., Boomer, I., Austin, P., Gates, J.B., Wang, N., Brooks, S., Zhang, J.: Moisture changes over the last millennium in arid central Asia: a review, synthesis and comparison with monsoon region, Quaternary Sci Rev, 29, 1055-1068, 2010.

Chen, F., Xu, Q., Chen, J., Birks, H.J.B., Liu, J., Zhang, S., Jin, L., An, C., Telford, R.J., Cao, X., Wang, Z., Zhang, X., Selvaraj, K., Lu, H., Li, Y., Zheng, Z., Wang, H., Zhou, A., Dong, G., Zhang, J., Huang, X., Bloemendal, J., Rao, Z.: East Asian summer monsoon precipitation variability since the last deglaciation, Sci Rep, 5, 11186, 2015.

Cheung, M.C., Zong, Y., Zheng, Z., Huang, K., Aitchinson, J.C.: A stable mid-Holocene monsoon climate of the central Tibetan Plateau indicated by a pollen record, Quatern Int, 333, 40-48, 2014.

Chikaraishi, Y.: $^{13}C/^{12}C$ signatures in plants and algae. In: Falkowski, E., Freeman, K.H. (eds.), Organic Geochemistry, Treatise on Geochemistry, 12, 95-123, 2014.

Clewing, C., Bössneck, U., von Oheimb, P.V., Albrecht, C.: Molecular phylogeny and biogeography of a high mountain bivalve fauna: The Sphaeriidae of the Tibetan Plateau, Malacologia, 56, 231-252, 2013.

Clewing, C., Riedel, F., Wilke, T., Albrecht, C.: Ecophenotypic plasticity leads to extraordinary gastropod shells found on the "Roof of the World", Ecology and Evolution, doi: 10.1002/ece3.1586, 2014a.

Clewing, C., von Oheimb, P.V., Vinarski, M., Wilke, T., Albrecht, C.: Freshwater mollusc diversity at the roof of the world: phylogenetic and biogeographical affinities of Tibetan Plateau *Valvata*, J Mollus Stud, 80, 452-455, 2014b.

Cloern, J.E., Canuel, E.A., Harris, D.: Stable carbon and nitrogen isotope composition of aquatic and terrestrial plants of the San Francisco estuarine system, Limnol Oceanogr, 47, 713-729, 2002.

Dartiguenave, C.: Arc Hydro: GIS in Water Resources, Environmental Systems Research Institute Press, Redlands, CA, 2007.

Demske, D., Tarasov, P.E., Wünnemann, B., Riedel, F.: Late glacial and Holocene vegetation, Indian monsoon and westerly circulation in the Trans-Himalaya recorded in the lacustrine pollen sequence from Tso Kar, Ladakh, NW India, Palaeogeogr Palaeocli, 279, 172-185, 2009.

Ding, J., Cuo, L., Zhang, Y., Zhu, F.: Monthly and annual temperature extremes and their changes on the Tibetan Plateau and its surroundings during 1963-2015, Sci Rep, 8, 11860, 2018.

Dortch, J.M., Owen, L.A., Caffee, M.W., Kamp, U.: Catastrophic partial drainage of Pangong Tso, northern India and Tibet, Geomorphology, 125, 109-121, 2011.

ESRI: Arc Hydro Tools v2.0 – Tutorial. Environmental Systems Research Institute Press, Redlands, CA, 2011.

ESRI: ArcGIS Desktop: Release 10.2. Environmental Systems Research Institute Press, Redlands, CA, 2013.

Fontes, J.C., Gasse, F., Gibert, E.: Holocene environmental changes in Lake Bangong basin (Western Tibet). Part 1: Chronology and stable isotopes of carbonates of a Holocene lacustrine core, Palaeogeogr Palaeocli, 120, 25-47, 1996.

Fontes, J.C., Mélières, F., Gibert, E., Liu, Q., Gasse, F.: Stable isotope and radiocarbon balances of two Tibetan lakes (Sumxi Co, Longmu Co) from 13,000 BP, Quaternary Sci Rev, 12, 875-887, 1993.

Frömming, E.: Biologie der mitteleuropäischen Süßwasserschnecken, Duncker & Humblot, Berlin, 1956.

Gajurel, A.P., France-Lanord, C., Huyghe, P., Guilmette, C., Gurung, D.: C and O isotope compositions of modern fresh-water mollusk shells and river waters from the Himalaya and Ganga plain, Chem Geol ,233, 156-183, 2006.

Gao, J., Yao, T., Joswiak, D.: Variations of water stable isotopes ($\delta^{18}O$) in two lake basins, southern Tibetan Plateau, Ann Glaciol, 55 doi: 10.3189/2014AoG66A109, 2014.

Gasse, F., Arnold, M., Fontes, J.C., Fort, M., Gibert, E., Huc, A., Li, Y., Liu, Q., Mélières, F., Van Campo, E., Wang, F., Zheng, Q.: A 13,000 yr climatic record in western Tibet, Nature 353, 742-745, 1991.

Gasse, F., Fontes, J.C., Van Campo, E., Wei, K.: Holocene environmental changes in Bangong Co basin (Western Tibet). Part 4: Discussion and conclusions, Palaeogeogr Palaeocli 120, 79-92.

Gasse, F., Van Campo, E., 1994. Abrupt post-glacial climate events in West Asia and North Africa monsoon domains, Earth Planet Sci Lett, 126, 435-456, 1996.

Gaten, E.: Life cycle of *Lymnaea peregra* (Gastropoda: Pulmonata) in the Leicester canal, U.K., with an estimate of annual production, Hydrobiologia, 135, 45-54, 1986.

Clim. Past Discuss., https://doi.org/10.5194/cp-2019-23
Manuscript under review for journal Clim. Past
Discussion started: 4 March 2019

Climate of the Past
Discussions

Gittenberger, E., Janssen, A.W., Kuijper, W.J., Kuiper, J.G.J., Meijer, T., van der Velde, G., de Vries, J.N.: De Nederlandse Zoetwatermollusken, Nationaal Natuurhistorisch Museum Naturalis, Leiden, 1998.

Glöer, P.: Die Süßwassergastropoden Nord- und Mitteleuropas, ConchBooks, Hackenheim, 2002.

Goto, A., Arakawa, H., Morinaga, H., Sakiyama, T.: The occurrence of hydromagnesite in bottom sediments from Lake Siling, central Tibet: implications for the correlation among $\delta^{18}O$, $\delta^{13}C$ and particle density, J Asian Earth Sci, 21, 979-988, 2003.

Gourbet, L., Mahéo, G., Leloup, P.H., Paquette, J.L., Sorrel, P., Henriquet, M., Liu, X., Liu, X.: Western Tibet relief evolution since the Oligo-Miocene, Gondwana Res, 41, 425-437, 2017.

Grün, R.: Electron spin resonance (ESR) dating. Quatern Int, 1, 98-109, 1989.

Guérin, G., Mercier, N., Adamiec, C.: Dose-rate conversion factors: update. Ancient TL 29, 5-8.

Harris, N., 2006. The elevation history of the Tibetan Plateau and its implications for the Asian monsoon, Palaeogeogr Palaeocli, 241, 4-15, 2011.

He, Y., Risi, C., Gao, J., Masson-Delmotte, V., Yao, T., Lai, C.T., Ding, Y., Worden, J., Frankenberg, C., Chepfer, H., Cesana, G.: Impact of atmospheric convection on south Tibet summer precipitation isotopologue composition using a combination of in situ measurements, satellite data, and atmospheric general circulation modeling, J of Geophys Res: Atmospheres, 120, 3852-3871, 2015.

Henderson, A.C.G., Holmes, J.A., Leng, M.J.: Late Holocene isotope hydrology of Lake Qinghai, NE Tibetan Plateau: effective moisture variability and atmospheric circulation changes, Quaternary Sci Rev, 29, 2215-2223, 2010.

Hillman, A.L., Abbott, M.B., Finkenbinder, M.S., Yu, J.Q.: An 8,600 year lacustrine record of summer monsoon variability from Yunnan, China, Quaternary Sci Rev, 174, 120-132, 2017.

Hren, M.T., Bookhagen, B., Blisniuk, P.M., Booth, A.L., Chamberlain, C.P.: $\delta^{18}O$ and δD of streamwaters across the Himalaya and Tibetan Plateau: Implications for moisture sources and paleoelevation reconstructions, Earth Planet Sci Lett, 288, 20-32, 2009.

Horton, T.W., Defliese, W.F., Tripati, A.K., Oze, C.: Evaporation induced ^{18}O and ^{13}C enrichment in lake systems: A global perspective on hydrologic balance effects, Quaternary Sci Rev, 131, 365-379, 2016.

Hou, J., D´Andrea, W.J., Wang, M., Ge, Y., Liang, J.: Influence of the Indian monsoon and the subtropical jet on climate change on the Tibetan Plateau since the late Pleistocene, Quaternary Sci Rev, 163, 84-94, 2017.

Hudson, A., Quade, J.: Long-term east-west asymmetry in monsoon rainfall on the Tibetan Plateau, Geology, 41, 351-354, 2013.

Hutchinson, G.E.: Limnological studies in Indian Tibet, Int Rev Hydrobiol, 35, 134-177, 1937.

Immerzeel, W., van Beck, L.P.H., Bierkens, M.F.P.: Climate change will affect the Asian water towers, Science, 328, 1382-1385, 2010.

Isozaki, Y., Kawahata, H., Ota, A.: A unique carbon isotope record across the Guadalupian-Lopingian (Middle-Upper Permian) boundary in mid-oceanic paleo-atoll carbonates: The high-productivity “Kamura event” and its collapse in Panthalassa, Global Planet Change, 55, 21-38, 2007.

Jacob, T., Wahr, J., Pfeffer, W.T., Swenson, S.: Recent contributions of glaciers and ice caps to sea level rise, Nature, 482, 514-518, 2012.

Jarvis, A., Reuter, H.I., Nelson, A., Guevara, E.: Hole-filled SRTM for the globe Version 4, available from the CGIAR-CSI SRTM 90m Database, http://srtm.csi.cgiar.org, 2008.

Killeen, I., Aldridge, D., Oliver, G.: Freshwater bivalves of Britain and Ireland. AIDGAP Occasional Publication 82, National Museum of Wales and Cambridge University, 2004.

Kong, P., Na, C., Fink, D., Huang, F.X., Ding, L.: Cosmogenic ^{10}Be inferred lake-level changes in Sumxi Co basin, Western Tibet, J Asian Earth Sci, 29, 698-703, 2007.

Kurita, N., Yamada, H.: The role of local moisture recycling evaluated using stable isotope data from over the Middle of the Tibetan Plateau during the monsoon season, J Hydromet, 9, 760-775, 2008.

Clim. Past Discuss., https://doi.org/10.5194/cp-2019-23
Manuscript under review for journal Clim. Past
Discussion started: 4 March 2019

Climate of the Past Discussions
Open Access

Kurita, N., Ichiyanagi, K., Matsumoto, J., Yamanaka, M.D., Ohata, T.: The relationship between the isotopic content of precipitation and the precipitation amount in tropical regions, J Geochem Explor, 102, 113-122, 2009.

Lee, J., Li, S.H., Aitchison, J.C.: OSL dating of paleoshorelines at Lagkor Tso, western Tibet, Quat Geochronol, 4, 335-343, 2009.

Lehmkuhl, F., Haselein, F.: Quaternary paleoenvironmental change on the Tibetan Plateau and adjacent areas (Western China and Western Mongolia), Quatern Int, 65/66, 121-145, 2000.

Lei, Y., Yao, T., Bird, B.W., Yang, K., Zhai, J., Sheng, Y.: Coherent lake growth on the central Tibetan Plateau since the 1970s: Characterization and attribution, J Hydrol, 483, 61-67, 2013.

Leipe, C., Demske, D., Tarasov, P.E., HIMPAC Project Members: A Holocene pollen record from the northwestern Himalayan lake Tso Moriri: Implications for palaeoclimatic and archaeological research, Quatern Int, 348, 93-112, 2013.

Leipe, C., Demske, D., Tarasov, P.E., Wünnemann, B., Riedel, F., HIMPAC Project members: Potential of pollen and non-pollen palynomorph records from Tso Moriri (Trans-Himalaya, NW India) for reconstructing Holocene limnology and human-environment interactions, Quatern Int, 348, 113-129, 2014.

Leng, M.J., Marshall, J.D.: Palaeoclimate interpretation of stable isotope data from lake sediment archives, Quaternary Sci Rev, 23, 811-831, 2004.

Li, H., Ku, T.: $\delta^{13}C$-$\delta^{18}O$ covariance as a paleohydrological indicator for closed-basin lakes, Palaeogeogr Palaeocli, 133, 69-80, 1997.

Liu, J., Wang, S., Yu, S., Yang, D., Zhang, L.: Climate warming and growth of high-elevation inland lakes on the Tibetan Plateau, Global Planet Change, 67, 209-217, 2009.

Liu, W., Zhang, P., Zhao, C., Wang, H., An, Z., Liu, H.: Reevaluation of carbonate concentration and oxygen isotope records from Lake Qinghai, the northeastern Tibetan Plateau, Quatern Int, 482, 122-130, 2018.

Liu, X., Lai, Z., Zeng, F., Madsen, D.B., E, C.: Holocene lake level variations on the Qinghai-Tibetan Plateau, Int J Earth Sci, 102, 2007-2016, 2013.

Clim. Past Discuss., https://doi.org/10.5194/cp-2019-23
Manuscript under review for journal Clim. Past
Discussion started: 4 March 2019

Liu, Y., Conrad, R., Yao, T., Gleixner, G., Claus, P.: Change of methane production pathway with sediment depth in a lake on the Tibetan plateau, Palaeogeogr Palaeocli, 474, 279-286, 2017.

Long, H., Haberzettl, T., Tsukamoto, S., Shen, J., Kasper, T., Daut, G., Zhu, L., Mäusbacher, R., Frechen, M.: Luminescence dating of lacustrine sediments from Tangra Yumco (southern Tibetan Plateau) using post-IR IRSL (pIRIR) signals from polymineral grains, Boreas, 44, 139-152, 2014.

Longbottom, T.L., Townsend-Small, A., Owen, L.A., Murari, M.K.: Climatic and topographic controls on soil organic matter storage and dynamics in the Indian Himalaya: Potential carbon cycle-climate change feedback, Catena, 119, 125-135, 2014.

Ma, R., Yang, G., Duan, H., Jiang, J., Wang, S., Feng, X., Li, A., Kong, F., Xue, B., Wu, J., Li, S.: China´s lakes at present: Number, area and spatial distribution, Science China Earth Sciences, 54, 283-289, 2011.

Mackelprang, R., Waldrop, M.P., DeAngelis, K.M., David, M.M., Chavarria, K.L., Blazewicz, S.J., Rubin, E.M., Jansson, J.K.: Metagenomic analysis of a permafrost microbial community reveals a rapid response to thaw, Nature, 480, 368-373, 2011.

Maussion, F., Scherer, D., Mölg, T., Collier, E., Curio, J., Finkelnburg, R.: Precipitation seasonality and variability over the Tibetan Plateau as resolved by the High Asia Reanalysis, J Climate, 27, 1910-1927, 2014.

Meier-Brook, C.: Substrate relations in some *Pisidium* species (Eulamellibranchiata: Sphaeriidae). Malacologia, 9, 121-125, 1969.

Meier-Brook, C.: Der ökologische Indikatorwert mitteleuropäischer *Pisidium*-Arten (Mollusca, Eulamellibranchiata), Eiszeitalter und Gegenwart, 26, 190-195, 1975.

Mischke, S., Herzschuh, U., Zhang, C., Bloemendal, J., Riedel, F.: A Late Quaternary lake record from the Qilian Mountains (NW China): lake level and salinity changes inferred from sediment properties and ostracod assemblages, Global Planet Change, 46, 337-359, 2005.

Mishra, P.K., Anoop, A., Jehangir, A., Prasad, S., Menzel, P., Schettler, G., Naumann, R., Weise, S., Andersen, N., Yousuf, A.R., Gaye, B.: Limnology and modern sedimentation patterns in high altitude Tso Moriri Lake, NW Himalaya – implications for proxy development, Fund Appl Limnol, 185, 329-348, 2014.

Mishra, P.K., Prasad, S., Anoop, A., Plessen, B., Jehangir, A., Gaye, B., Menzel, P., Weise, S.M., Yousuf, A.R.: Carbonate isotopes from high altitude Tso Moriri (NW Himalayas) provide clues to late glacial and Holocene moisture source and atmospheric circulation changes, Palaeogeogr Palaeocli, 425, 76-83, 2015.

Molnar, P., Boos, W.R., Battisti, D.S.: Orographic controls on climate and paleoclimate of Asia: Thermal and Mechanical Roles for the Tibetan Plateau, Ann Rev Earth Planet Sci, 38, 77-102, 2009.

Morrill, C., Overpeck, J.T., Cole, J.E., Liu, K., Shen, C., Tang, L.: Holocene variations in the Asian monsoon inferred from the geochemistry of lake sediments in central Tibet, Quaternary Res, 65, 232-243, 2006.

NASA Landsat Program: Landsat ETM+scene LE71460372012267PFS00, SLC-Off, USGS, Sioux Falls, 2012/09/23.

NASA Landsat Program: Landsat ETM+scene LE71450372012260PFS00, SLC-Off, USGS, Sioux Falls, 2012/09/16.

Økland, J.: Lakes and snails. Backhuys, Oegstgeest, 1990.

Økland, K.A., Kuiper, J.G.J.: Distribution of small mussels (Sphaeriidae) in Norway with notes on their ecology, Malacologia, 22, 469-477, 1982.

Oppermann, F., Tsukamoto, S.: A portable system of X-ray irradiation and heating for electron spin resonance (ESR) dating. Ancient TL, 33, 11-15, 2015.

Ou, Y.: Hydrological characteristics of the east Bangong Lake. In: Environment and ecology of Qinghai-Xizang Plateau, Science Press, Beijing, 1713-1717, 1981.

Pande, K., Padia, J.T., Ramesh, R., Sharma, K.K.: Stable isotope systematics of surface water bodies in the Himalayan and Trans-Himalayan (Kashmir) region, P Indian Acad Sc, 109, 109-115, 2000.

Prescott, J.R., Hutton, J.T.: Cosmic ray contributions to dose rates for luminescence and ESR dating: large depths and long-term time variations, Radiat Meas, 23, 497-500, 1994.

Clim. Past Discuss., https://doi.org/10.5194/cp-2019-23
Manuscript under review for journal Clim. Past
Discussion started: 4 March 2019

Qiang, M., Song, L., Jin, Y., Li, Y., Liu, L., Zhang, J., Zhao, Y., Chen, F.: A 16-ka oxygen-isotope record from Genggahai Lake on the northwestern Qinghai-Tibetan Plateau: Hydroclimatic evolution and changes in atmospheric circulation, Quaternary Sci Rev, 162, 72-87, 2017.

Ramisch, A., Lockot, G., Haberzettl, T., Hartmann, K., Kuhn, G., Lehmkuhl, F., Schimpf, S., Schulte, P., Stauch, G., Wang, R., Wünnemann, B., Yan, D., Zhang, Y., Diekmann, B.: A persistent northern boundary of Indian Summer Monsoon precipitation over Central Asia during the Holocene, Sci Rep, 6, 25791, 2016.

Ran, Y., Li, X., Jin, R., Guo, J.: Remote sensing of the mean annual surface temperature and surface frost number for mapping permafrost in China, Arc Antarc Alp Res, 47, 255-265, 2015.

Rivkina, E., Shcherbakova, V., Laurinavichius, K., Petrovskaya, L., Krivushin, K., Kraev, G., Pecheritsina, S., Gilichinsky, D.: Biogeochemistry of methane and methanogenic archaea in permafrost, FEMS Microbiol Ecol, 61, 1-15, 2007.

Schellmann, G., Beerten, K., Radtke, U.: Electron spin resonance (ESR) dating of Quaternary materials, Quaternary Sci J, 57, 150-178, 2008.

Shi, X., Kirby, E., Furlong, K.P., Meng, K., Robinson, R., Lu, H., Wang, E.: Rapid and punctuated Late Holocene recession of Siling Co, central Tibet, Quaternary Sci Rev, 172, 15-31, 2017.

Shi, Y., Yu, G., Liu, X., Li, B., Yao, T.: Reconstruction of the 30-40 ka BP enhanced Indian monsoon climate based on geological records from the Tibetan Plateau, Palaeogeogr Palaeocli, 169, 69-83, 2007.

Skinner, A.F.: ESR dosimetry and dating in aragonitic mollusks, Appl Rad Isot, 40, 1081-1085, 1989.

Stiller, M., Rounick, J.S., Shasha, S.: Extreme carbon isotope-enrichments in evaporating brines, Nature, 316, 434-435, 1985.

Stuiver, M., Reimer, P. J., Reimer, R. W.: CALIB 7.0. Radiocarbon calibration, http://calib.qub.ac.uk/calib/calib.html, 2013.

Taft, L., Mischke, S., Wiechert, U., Leipe, C., Rajabov, I., Riedel, F.: Sclerochronological oxygen and carbon isotope ratios in *Radix* (Gastropoda) shells indicate changes of glacial meltwater flux and temperature since 4,200 cal yr BP at Lake Karakul, eastern Pamirs (Tajikistan), J Paleolim, 52, 27-41, 2014.

Clim. Past Discuss., https://doi.org/10.5194/cp-2019-23
Manuscript under review for journal Clim. Past
Discussion started: 4 March 2019

Climate of the Past Discussions

Taft, L., Wiechert, U., Riedel, F., Weynell, M., Zhang, H.: Sub-seasonal oxygen and carbon isotope variations in shells of modern *Radix* sp. (Gastropoda) from the Tibetan Plateau: Potential of a new archive for palaeoclimatic studies, Quaternary Sci Rev, 34, 44-56, 2012.

Taft, L., Wiechert, U., Zhang, H., Lei, G., Mischke, S., Plessen, B., Weynell, M., Winkler, A., Riedel, F.: Oxygen and carbon isotope patterns archived in shells of the aquatic gastropod *Radix*: Hydrologic and climatic signals across the Tibetan Plateau in sub-monthly resolution, Quat Int, 290-291, 282-298, 2013.

Tian, L., Yao, T., MacClune, K., White, J.W.C., Schilla, A., Vaughn, B., Vachon, R., Ichiyanagi, K.: Stable isotope variations in west China: A consideration of moisture sources, J Geophys Res, 112, D10112, 2007.

Turner, H., Kuiper, J.G.J., Thew, N., Bernasconi, R., Rüetschi, J., Wüthrich, M., Gosteli, M.: Atlas der Mollusken der Schweiz und Liechtensteins, Fauna Helvetica 2. CSCF and SEG, Neuchâtel, 1989.

Van Campo, E., Gasse, F.: Pollen- and diatom-inferred climatic and hydrological changes in Sumxi Co basin (Western Tibet) since 13,000 yr B.P, Quatern Res, 39, 300-313, 1993.

Wagner, D., Gattinger, A., Embacher, A., Pfeiffer, E.M., Schloter, M., Lipski, A.: Methanogenic activity and biomass in Holocene permafrost deposits of the Lena Delta, Siberian Arctic and its implication for the global methane budget, Glob Change Biol, 13, 1089-1099, 2007.

Walter, K.M., Zimov, S.A., Chanton, J.P., Verbyla, D., Chapin III, F.S.: Methane bubbling from Siberian thaw lakes as a positive feedback to climate warming, Nature, 443, 71-75, 2006.

Wang, B., French, H.M.: Permafrost on the Tibet Plateau, China, Quaternary Sci Rev, 14, 255-274, 1995.

Wang, C., Hu, K., eds.: Geological map of Qinghai-Xizang (Tibet) Plateau and adjacent areas, Chengdu Cartographic Publishing House, China, 2004.

Wang, M., Hou, J., Lei, Y.: Classification of Tibetan lakes based on variations in seasonal lake water temperature, Chin Sci Bull, 59, 4847-4855, 2014.

Wang, Y., Liu, X., Herzschuh, U.: Asynchronous evolution of the Indian and East Asian Summer Monsoon indicated by Holocene moisture patterns in monsoonal central Asia, Earth Sci Rev, 103, 135-153, 2010.

Walker, M.J.C., Berkelhammer, M., Björck, S., Cwynar, L.C., Fisher, D.A., Long, A.J., Lowe, J.J., Newnham, R.M., Rasmussen, S.O., Weiss, H.: Formal subdivision of the Holocene Series/Epoch: a discussion paper by a working group of INTIMATE (Integration of ice-core, marine and terrestrial records) and the Subcommission on Quaternary Stratigraphy (International Commission on Stratigraphy), J Quatern Sci, 27, 649-659, 2012.

Wassermann, N.: Quantitative Bestimmung der Haupt- und Spurenelementgehalte von biogenen Karbonaten mittels Plasmaquellen-Massenspektrometrie (ICP-MS), Unpublished B.Sc. thesis, Freie Universität Berlin, 2014.

Wei, K., Gasse, F.: Oxygen isotopes in lacustrine carbonates of West China revisited: implications for post glacial changes in summer monsoon circulation, Quatern Sci Rev, 18, 1315-1334, 1999.

Wei, J., Liu, S., Guo, W., Xu, J., Bao, W., Shangguan, D.: Changes in glacier volume in the north bank of the Bangong Co Basin from 1968 to 2007 based on historical topographic maps, SRTM, and ASTER stereo images, Arc Antarc Alp Res, 47, 301-311, 2015.

Wen, R., Tian, L., Liu, F., Qu, D.: Lake water isotope variation linked with the in-lake water cycle of the alpine Bangong Co, arid western Tibetan Plateau, Arc Antarc Alp Res, 48, 563-580, 2016.

Wilckens, F.K.: On the origin of magnesium isotope variation in waters and sediments of Lake Bangong, Tibet autonomous region of China, Unpublished master thesis, Freie Universität Berlin, 2014.

Wünnemann, B., Reinhardt, C., Kotlia, B.S., Riedel, F.: Observations on the relationship between lake formation, permafrost activity and Lithalsa development during the last 20000 years in the Tso Kar Basin, Ladakh, India, Permafr Perigl Proc, 19, 341-358, 2008.

Wünnemann, B., Demske, D., Tarasov, P., Kotlia, B.S., Reinhardt, C., Bloemendal, J., Diekmann, B., Hartmann, K., Krois, J., Riedel, F., Arya, N.: Hydrological evolution during the last 15 kyr in the Tso Kar lake basin (Ladakh, India), derived from geomorphological, sedimentological and palynological records, Quaternary Sci Rev, 29, 1138-1155, 2010.

Wünnemann, B., Yan, D., Andersen, N., Riedel, F., Zhang, Y., Sun, Q., Hoelzmann, P.: A 14 ka high-resolution $\delta^{18}O$ lake record reveals a paradigm shift for the process-based reconstruction of hydroclimate on the northern Tibetan Plateau, Quaternary Sci Rev, 200, 65-84, 2018.

Clim. Past Discuss., https://doi.org/10.5194/cp-2019-23
Manuscript under review for journal Clim. Past
Discussion started: 4 March 2019

Wynn, J.G.: Carbon isotope fractionation during decomposition of organic matter in soils and paleosols: Implications for paleoecological interpretations of paleosols, Palaeogeogr Palaeocli, 251, 437-448, 2007.

Yao, T., Masson-Delmotte, V., Gao, J., Yu, W., Yang, X., Risi, C., Sturm, C., Werner, M., Zhao, H., He, Y., Ren, W., Tian, L., Shi, C., Hou, S.: A review of climatic controls on $\delta^{18}O$ in precipitation over the Tibetan Plateau: Observations and simulations, Rev Geophy, 51, 525-548, 2013.

Yu, G., Harrison, S.P., Xue, B.: Lake status records from China: Data Base Documentation. Technical Report 4. Max Planck Institute for Biogeochemistry Jena, Germany, http://www.bgc-jena.mpg.de/uploads/Publications/TechnicalReports/tech_report4.pdf, 2001.

Yu, W., Yao, T., Tian, L., Ma, Y., Kurita, N., Ichiyanagi, K., Wang, Y., Sun, W.: Stable isotope variations in precipitation and moisture trajectories on the western Tibetan Plateau, China, Arc Antarc Alp Res, 39, 688-693, 2007.

Zettler, M.L., Jueg, U., Menzel-Harloff, H., Göllnitz, U., Petrick, S., Weber, E., Seemann, R.: Die Land- und Süßwassermollusken Mecklenburg-Vorpommerns, Obotritendruck, Schwerin, 2006.

Zhang, G., Xie, H., Kang, S., Yi, D., Ackley, S.F.: Monitoring lake level changes on the Tibetan Plateau using ICESat altimetry data (2003-2009), Remote Sens Environ, 115, 1733-1742, 2011.

Zheng, M.: An introduction to saline lakes on the Qinghai-Tibet Plateau, Kluwer Academic Publishers, Dordrecht, 1997.

Zhu, Z., Chen, J., Zeng, Y.: Abnormal positive $\delta^{13}C$ values of carbonate in Lake Caohai, southwest China, and their possible relation to lower temperature, Quat Int, 286, 85-93, 2013.

Figure captions

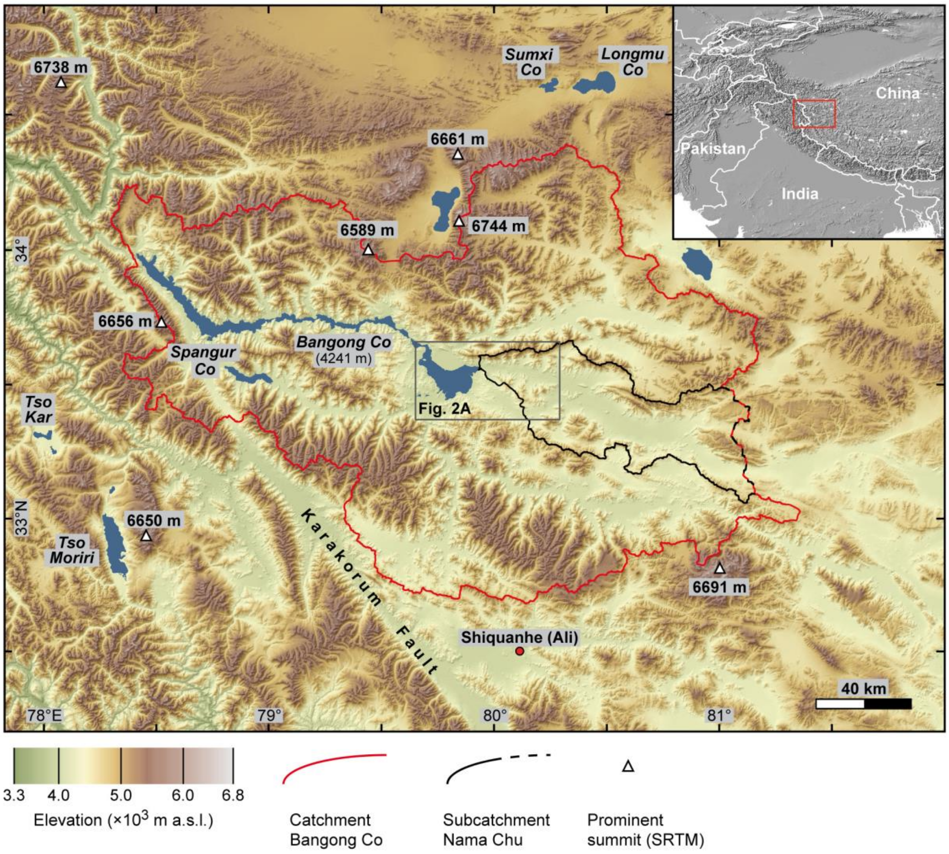

1046

1047 **Fig. 1.** Digital elevation model (SRTM) of part of the western Tibetan Plateau showing the transboundary Bangong Co drainage basin with lake system, total catchment (red line) and sub-catchment of Nama Chu valley (black line). All elevations are derived from SRTM.

Clim. Past Discuss., https://doi.org/10.5194/cp-2019-23
Manuscript under review for journal Clim. Past
Discussion started: 4 March 2019

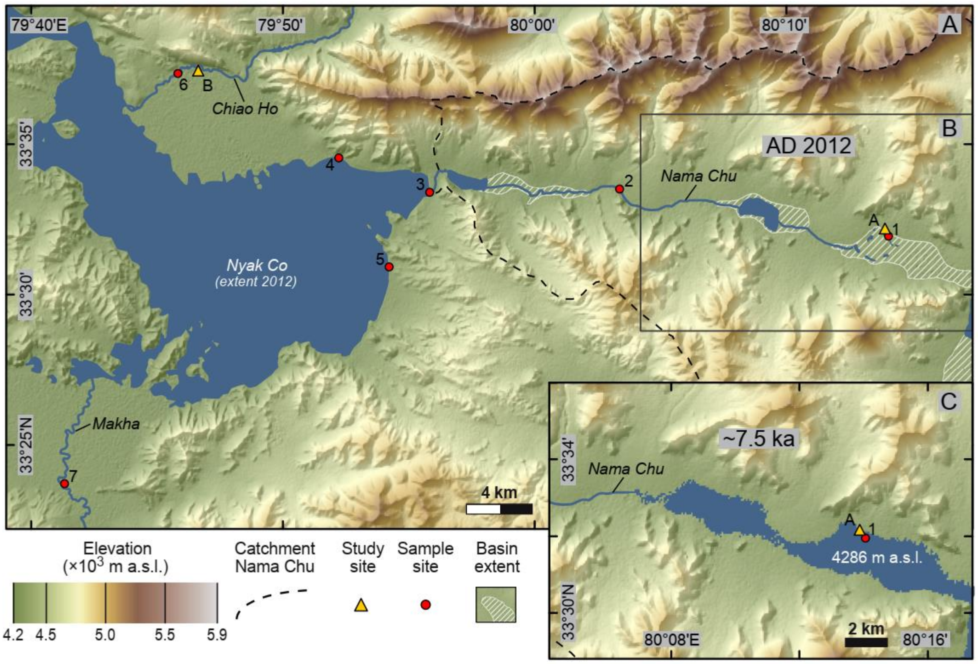

1050

1051 **Fig. 2. A.** Digital elevation model (SRTM) of the eastern Bangong Co system (Nyak Co) with
1052 locations of water samples, study sites and major tributaries indicated by symbols. **B.** Focal area as in
1053 2012. **C.** Water extension of focal area simulated for ~7.5 ka, based on the morphology of basins,
1054 palaeo-shorelines and the altitudinal position of fossil shell bearing fluvio-lacustrine sediments.

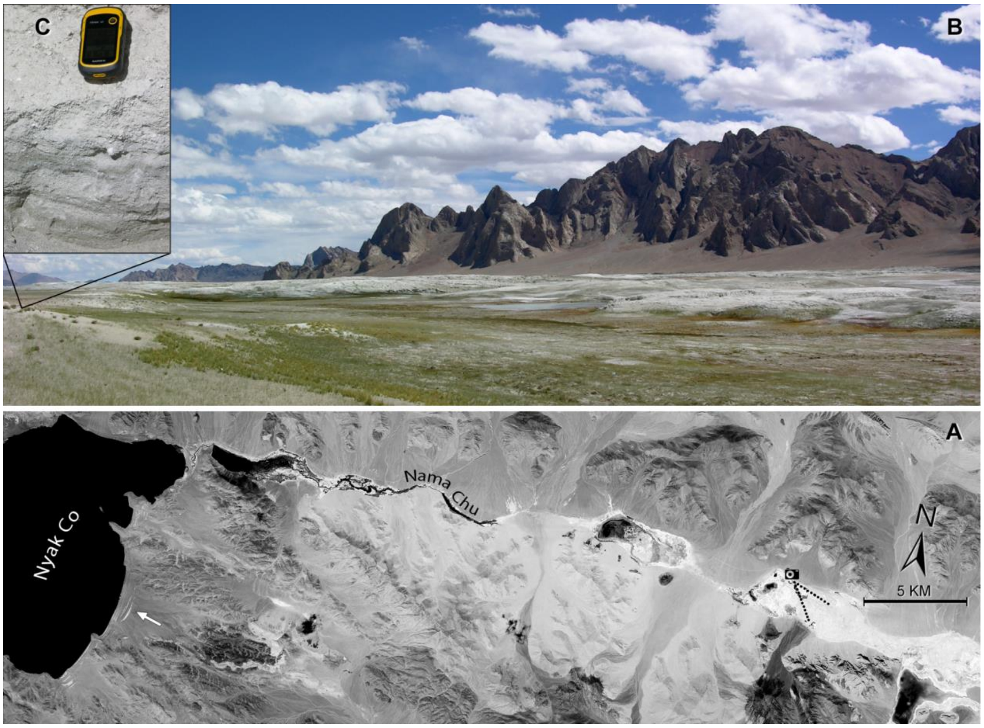

Fig. 3. A. CORONA satellite image of western Nama Chu valley and Nyak Co, the easternmost lake basin of the Bangong Co system (compare Fig. 1); arrow: palaeo-shoreline features. Camera symbol and dotted lines refer to figure 3B; **B.** Photograph taken in September 2012 showing the modern setting of the studied palaeo-hydrological system in Nama Chu valley; the greyish undulated landscape between the grassland and the mountains represents frozen mounds of lacustrine sediments, formed by permafrost processes; **C.** Littoral sediments of ~7.5 ka age, from which the studied molluscan shells were sampled (Handheld GPS for scale); the sediments were found along a palaeo-shoreline.

Clim. Past Discuss., https://doi.org/10.5194/cp-2019-23
Manuscript under review for journal Clim. Past
Discussion started: 4 March 2019

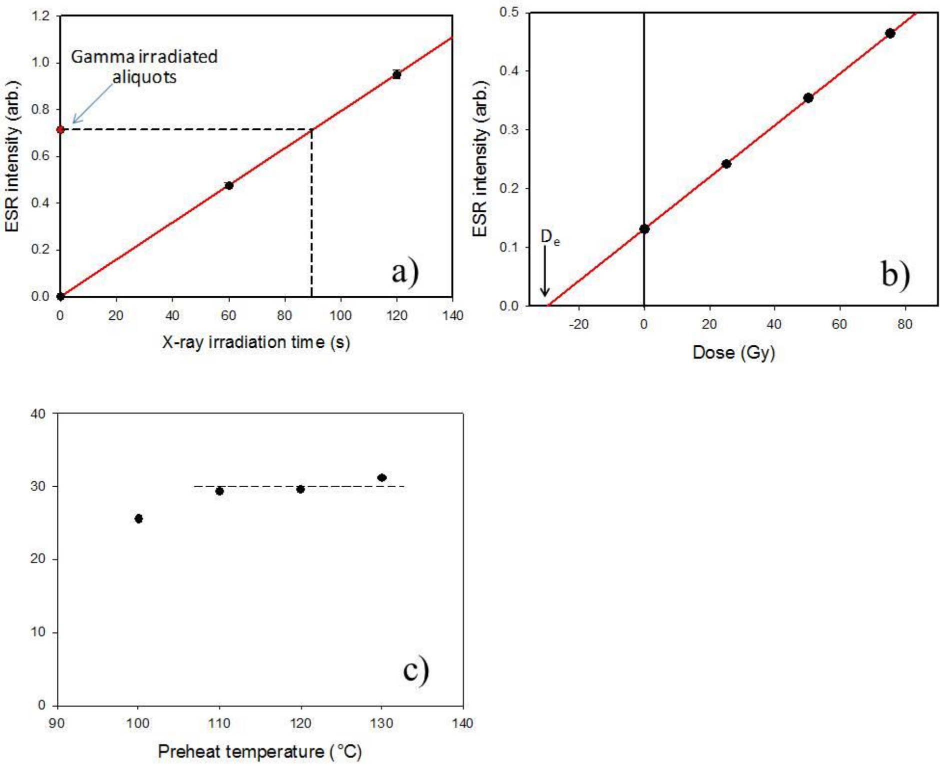

Fig. 4. A. X-ray calibration of calcium carbonate using a modern coral sample. Each data point is the mean of 3 aliquots. **B.** Single aliquot additive dose D_e measured from one aliquot of *Radix* shell preheated at 120°C. **C.** D_e values of the *Radix* shell sample measured at different preheat temperatures.

Fig. 5. One (NC2) of the five (NC1-5) fossil *Radix* sp. shells from Nama Chu valley, which were sub-sampled sclerochronologically for stable isotope analyses.

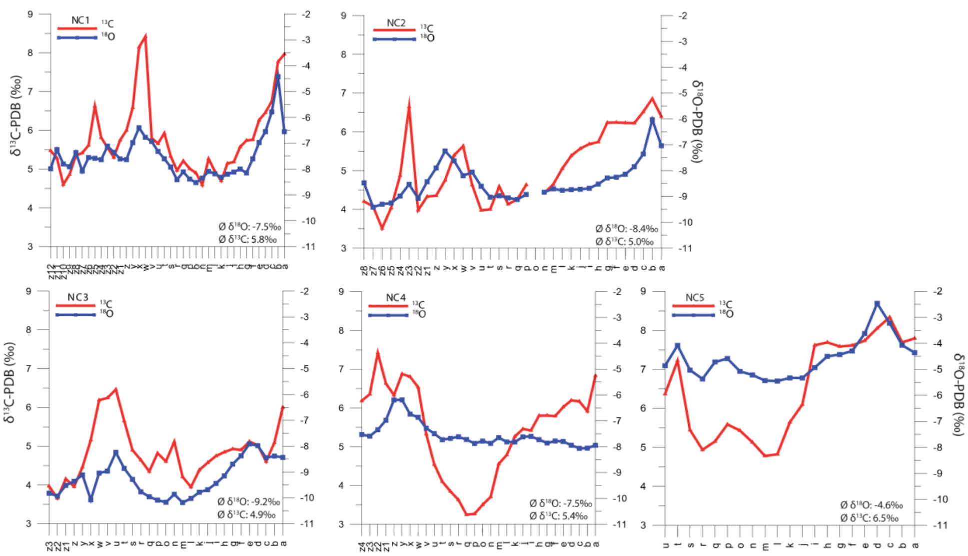

Fig. 6. Sclerochronological $\delta^{18}O$ and $\delta^{13}C$ patterns from studied early Middle Holocene *Radix* sp. shells (NC1-NC5) sampled from Nama Chu valley sediments.

Table captions

Table 1. Selected water parameters from Nyak Co (3-5) and two tributaries (6 and 7) and from Nama Chu (1 and 2). Except for electric conductivity, psu, T and pH, all analytical data from Wilckens (2014). Location numbers refer to Fig. 2.

Map location	1	2	3	4	5	6	7
Geographical	33.5326°N	33.5581°N	33.5573°N	33.5767°N	33.5152°N	33.6219°N	
	33.3945°N						
coordinates	80.2346°E	80.0558°E	79.9319°E	79.8695°E	79.9043°E	79.7633°E	
	79.6880°E						
Sampling date	16.09.2012	16.09.2012	11.09.2012	14.09.2012	11.09.2012	14.09.2012	
	17.09.2012						
Water T in °C	20.2	23.3	13.8	19.2	18.2	13.3	11.2

Clim. Past Discuss., https://doi.org/10.5194/cp-2019-23
Manuscript under review for journal Clim. Past
Discussion started: 4 March 2019

EC µS/cm	41600	731	786	909	920	555	239
psu	29.89	0.37	0.51	0.51	0.53	0.35	0.16
pH	8.8	8.4	9.3	9.3	8.9	8.8	8.5
$\delta^{18}O_W$ ‰	n.a.	-13.0	-8.4	-3.9	-3.5	-13.9	-13.3
δD_W ‰	n.a.	-91.5	-75.7	-48.8	-48.6	-100.2	-99.3
$\delta^{13}C_{DIC}$ ‰	+6.2	+0.7	+0.1	+2.4	+2.2	-1.0	-6.5
HCO_3 µmol/l	22786	4827	3327	4338	5390	3686	1875
SO_4 µmol/l	55164	916	1343	999	895	531	135
Na µmol/l	154539	2540	3741	4741	4654	1662	557
Cl µmol/l	n.a.	1439	2200	2821	2933	1015	296
Ca µmol/l	1241	1347	599	439	482	1332	586
Mg µmol/l	34584	1399	1917	2292	2218	876	407
K µmol/l	4617	113	143	624	223	74	49
B µmol/l	11962	88	125	312	300	76	120

Table 2. AMS radiocarbon dates of three fossil *Radix* sp. shells and of two charcoal samples.

Site/Sample ID	Material	^{14}C-age yr BP	Res. corrected age cal. yr BP	Laboratory ID
Chiao Ho 34-36 S	Radix shell	8540 ± 40	2211 ± 55	Poz-53269
Chiao Ho 40-42 S	Radix shell	8480 ± 40	2428 ± 85	Poz-53271
Chiao Ho 34-36 C	Charcoal	2275 ± 30	2275 ± 30	Poz-53314
Chiao Ho 40-42 C	Charcoal	2400 ± 30	2400 ± 35	Poz-53315
Nama Chu	Radix shell	12670 ± 60	7393 ± 114	Poz-53277

Table 3. Dose rate, equivalent dose and ESR age.

Table 3: Dose rate, equivalent dose and ESR age.

^{238}U (Bq/kg)	27.6	±	1.5	Internal U (ppm)*	2.8	±	2.7
^{226}Ra (Bq/kg)	14.6	±	0.3	Internal dose rate (Gy/ka), early uptake	0.66	±	0.46
^{232}Th (Bq/kg)	18.4	±	0.2	Internal dose rate (Gy/ka), linear uptake	0.33	±	0.33
K (Bq/kg)	687	±	5	Total dose rate (Gy/ka), early uptake	3.97	±	0.49
External dose rate (Gy/ka)	2.91	±	0.21	Total dose rate (Gy/ka), linear uptake	3.64	±	0.41
Cosmic dose rate (Gy/ka)	0.40	±	0.04	Age, early uptake (ka)	7.4	±	1.0
D_e (Gy)	29.5	±	1.1	Age, linear uptake (ka)	8.1	±	1.0

* mean value of Holocene shells (Schellmann et al., 2008).

Table 4. Classification, and biological and ecological traits of early Middle Holocene molluscs from the study area using the best modern analogue approach. Compiled from Burky et al., 1981; Clewing et al., 2013, 2014a, 2014b; Frömming, 1956; Gittenberger et al., 1998; Glöer, 2002; Killeen et al., 2004; Meier-Brook, 1969, 1975; Økland and Kuiper, 1982; Økland, 1990; Taft et al., 2012, 2013; Turner et al., 1998; Wilckens, 2014; Zettler et al., 2006; and personal observations.

Taxon	*Radix* sp.	*Gyraulus* sp.	*Valvata* sp.	*Pisidium* sp.
Classification	Gastropoda, Basommatophora, Lymnaeidae	Gastropoda, Basommatophora, Planorbidae	Gastropoda, Allogastropoda, Valvatidae	Bivalvia, Veneroida, Sphaeriidae
Life span (years)	0.5-1.5	1-1.5	1-2	0.5-3
Salinity range	freshwater to meso-haline (≤ 14 psu)	freshwater to oligo-haline (≤ 5 psu)	freshwater to oligo-haline (≤ 5 psu)	freshwater to oligo-haline (≤ 3 psu)
pH range	5.2-10.4	5.0-10.4	5.0-9.6	4.0-9.3
Aquatic system	wetlands, fluvial and lacustrine systems (moderate water movement preferred)	fluvial and lacustrine systems (still water conditions preferred)	fluvial and lacustrine systems (still to slow moving water conditions preferred)	wetlands, fluvial and lacustrine systems (moderate water movement preferred)
Water depth	most common in shallow littoral (ca. 0.1-2 m)	most common in shallow littoral (ca. 0.1-2 m)	most common in littoral (1.5-3 m)	most common in shallow littoral (ca. 0.1-2 m)
Substrate	epibenthic on all kinds of substrates (e.g. pebbles, sand, gyttja, water plants)	epibenthic on different solid substrates (e.g. pebbles, water plants) and on gyttja	epibenthic on all kinds of substrates (preferably organic-rich sediment)	endo- or epibenthic; soft substrates (most common in/on organic-rich silt and fine sand)

Clim. Past Discuss., https://doi.org/10.5194/cp-2019-23
Manuscript under review for journal Clim. Past
Discussion started: 4 March 2019

Climate of the Past Discussions

Table 5. Size parameters and number of sub-samples of *Radix* shells used for stable isotope analyses.

Sample ID	Height in cm	N whorls	N sub-samples
NC1	1.59	4.6	38
NC2	1.34	5.1	34
NC3	1.39	5	29
NC4	1.49	4.8	30
NC5	1.28	3.6	21

Table 6. $\delta^{13}C$ and $\delta^{18}O$ values from the five selected *Radix* shells NC1-5. Letter "a" indicates the sub-sample from the outer rim of the aperture and thus the latest/youngest shell in ontogeny. The last letters are mostly combined with numbers and vary due to the different sizes of the shells and corresponding differences in maximum sub-sample numbers and represent the earliest (embryonic) and thus oldest shell in ontogeny (z12, z8, z3, z4, u). Data are presented in individual graphs in Fig. 6.

	NC1		NC2		NC3		NC4		NC5	
	$\delta^{13}C$	$\delta^{18}O$	$\delta^{13}C$	$\delta^{18}O$	$\delta^{13}C$	$\delta^{18}O$	$\delta^{13}C$	$\delta^{18}O$	$\delta^{13}C$	$\delta^{18}O$
a	8.0	-6.6	6.4	-7.0	6.0	-8.4	6.8	-7.9	7.8	-4.4
b	7.8	-4.4	6.9	-6.0	5.1	-8.4	5.9	-8.1	7.7	-4.1
c	6.7	-5.8	6.5	-7.4	4.6	-8.4	6.2	-8.1	8.3	-3.2
d	6.5	-6.6	6.2	-7.9	5.0	-8.0	6.2	-7.9	8.1	-2.5
e	6.3	-7.0	6.2	-8.1	5.1	-7.9	6.0	-7.8	7.7	-3.6
f	5.8	-7.6	6.2	-8.3	4.9	-8.4	5.8	-7.8	7.6	-4.3
g	5.7	-8.1	6.2	-8.3	4.9	-8.7	5.8	-7.9	7.6	-4.4
h	5.6	-8.0	5.7	-8.5	4.8	-9.2	5.8	-7.7	7.7	-4.5
i	5.2	-8.1	5.7	-8.7	4.7	-9.4	5.4	-7.6	7.6	-4.9
j	5.1	-8.2	5.6	-8.7	4.6	-9.7	5.5	-7.6	6.1	-5.3
k	4.7	-8.3	5.4	-8.7	4.4	-9.8	5.3	-7.8	5.6	-5.3
l	4.9	-8.2	5.1	-8.8	3.9	-10.0	4.8	-7.8	4.8	-5.5
m	5.3	-8.1	4.6	-8.7	4.2	-10.2	4.6	-7.6	4.8	-5.4
n	4.6	-8.3	4.4	-8.8	5.1	-9.9	3.7	-7.9	5.1	-5.2
o	4.9	-8.5	4.4	-6.5	4.6	-10.2	3.5	-7.8	5.4	-5.1
p	5.0	-8.4	4.6	-8.9	4.8	-10.1	3.3	-7.9	5.6	-4.6
q	5.2	-8.1	4.3	-9.1	4.3	-10.0	3.2	-7.7	5.2	-4.7
r	5.0	-8.4	4.1	-9.1	4.6	-9.8	3.6	-7.6	4.9	-5.4
s	5.3	-7.9	4.6	-9.0	4.9	-9.3	3.8	-7.7	5.4	-5.0
t	5.9	-7.6	4.0	-9.0	5.7	-8.9	4.1	-7.7	7.2	-4.1
u	5.7	-7.3	4.0	-8.6	6.5	-8.2	4.5	-7.5	6.4	-4.9
v	5.8	-6.9	4.6	-8.1	6.2	-9.0	5.3	-7.3		
w	8.4	-6.8	5.6	-8.2	6.2	-9.0	6.5	-6.9		
x	8.1	-6.4	5.4	-7.6	5.2	-10.1	6.8	-6.7		
y	6.6	-7.0	4.8	-7.2	4.5	-9.1	6.9	-6.2		
z	6.0	-7.6	4.4	-7.9	4.0	-9.4	6.3	-6.2		
z1	5.7	-7.6	4.3	-8.4	4.2	-9.5	6.6	-7.0		
z2	5.3	-7.4	4.0	-9.1	3.7	-9.9	7.4	-7.3		

Clim. Past Discuss., https://doi.org/10.5194/cp-2019-23
Manuscript under review for journal Clim. Past
Discussion started: 4 March 2019

z3	5.6	-7.1	6.6	-8.5	4.0	-9.8	6.4	-7.6		
z4	5.8	-7.6	4.9	-9.0			6.2	-7.5		
z5	6.6	-7.6	4.0	-9.3						
z6	5.6	-7.6	3.5	-9.3						
z7	5.4	-8.1	4.1	-9.4						
z8	5.3	-7.4	4.2	-8.5						
z9	4.9	-7.9								
z10	4.6	-7.8								
z11	5.3	-7.2								
z12	5.5	-8.0								
Ø	5.8	-7.5	5.1	-8.4	4.9	-9.3	5.4	-7.5	6.5	-4.6